

***A MODEL STUDY OF BOCA CIEGA BAY, JOHN'S PASS, AND BLIND PASS***

**by**

***MAY LING BECKER and MARK A. ROSS***



Publication Report:  
No. CMHAS.FDOT.99.01

July 1999

Center for Modeling Hydrologic and Aquatic Systems  
Department of Civil and Environmental Engineering  
University of South Florida  
Tampa, Florida

## ACKNOWLEDGMENTS

The authors acknowledge and appreciate the financial support provided by the Florida Department of Transportation. Also, information and data provided by Pitman-Hartenstein & Associates and Ayers Associates is acknowledged.

## TABLE OF CONTENTS

LIST OF TABLES .....	iii
ILLUSTRATIONS .....	iv
SUMMARY .....	vi
INTRODUCTION .....	1
Objectives .....	1
Study Area .....	4
BACKGROUND .....	7
Evolution of Boca Ciega Bay .....	7
John’s Pass .....	9
Blind Pass .....	11
Methods Used to Evaluate Stability of John’s Pass and Blind Pass .....	13
Empirical Relationships .....	13
Ratios of Tidal Prism to Littoral Drift .....	14
Stability Diagrams .....	14
CONSTRUCTION OF THE NUMERICAL MODEL .....	16
Field Study .....	16
Tidal Heights .....	16
Velocities .....	18
Bathymetric Transects .....	18
Computer Model .....	20
Construction of Boca Ciega Bay Model .....	20
Boca Ciega Bay Model Calibration .....	22
Tides .....	22
Additional Constrictions .....	22
Flow Simulation of Boca Ciega Bay .....	23
Storm-Surge Simulation of Boca Ciega Bay .....	23
RESULTS OF CALIBRATION .....	24
Peak Velocities .....	27
Discharge and Cumulative Volumes .....	27

Net Flow .....	31
Peak Velocities Resulting from Storm-surge Simulation .....	32
STABILITY OF THE PASSES .....	33
Empirical Relationships .....	33
Ratios of Tidal Prism to Littoral Drift .....	35
Stability Diagrams from Predictive Simulations .....	36
Flow Regime of Boca Ciega Bay .....	44
Stability of John’s Pass .....	44
Stability of Blind Pass .....	45
HYDRAULIC EVOLUTION OF BOCA CIEGA BAY .....	46
CONCLUSIONS .....	49
REFERENCES .....	51
APPENDICES .....	53
Appendix A. Section of Input Data Set .....	54
Appendix B. Spring-tide Calibration Results .....	61
Appendix C. Neap-tide Calibration Results .....	65
Appendix D. Channel Velocities at John’s Pass and Blind Pass .....	69
Appendix E. Discharge, Volume, and Net Flow at Boundary Channels .....	70

## LIST OF TABLES

1. History of John's Pass .....	10
2. History of Blind Pass .....	12
3. Stability index proposed by Bruun (1978) .....	14
4. Peak channel velocities at John's Pass and Blind Pass .....	27
5. Net flow for 11-day simulation .....	31
6. Tidal prism of channels serving Boca Ciega Bay .....	32

## ILLUSTRATIONS

1. Boca Ciega Bay study area .....	3
2. History of cross-sectional areas of John's Pass and Blind Pass (adapted from CPE, 1992) .....	5
3. Escoffier's stability concept (after O'Brien and Dean, 1972) .....	15
4. Location of tide gauges and bathymetric transects in the Boca Ciega Bay study area .....	17
5. Location of velocity stations in the Boca Ciega Bay study area. ....	19
6. Grid array of the Boca Ciega Bay model .....	21
7. Results of spring-tide model calibration at John's Pass and Blind Pass. ....	25
8. Results of neap-tide model calibration at John's Pass and Blind Pass .....	26
9. Discharge, volume, and net flow of Boca Ciega Bay as a result of the 11-day flow simulation .....	29
10. Discharge, volume, and net flow at John's Pass and Blind Pass as a result of the 11-day flow simulation .....	30
11. Jarrett's (1976) area versus prism regression analysis and tidal prism values for John's Pass and Blind Pass produced by the Boca Ciega Bay model .....	34
12. Stability diagram for Blind Pass and corresponding maximum velocities at John's Pass. ....	38
13. Tidal prisms of Blind Pass and John's Pass as a result of changes in the cross-sectional area of Blind Pass. ....	39
14. Tidal prism of Boca Ciega Bay as a result of changes in the cross-sectional area of Blind Pass. ....	40

15. Stability diagram for Johns' Pass and corresponding maximum velocities at Blind Pass .....	41
16. Tidal prisms of Blind Pass and John's Pass as a result of changes in the cross-sectional area of John's Pass. ....	42
17. Tidal prism of Boca Ciega Bay as a result of changes in the cross-sectional area of John's Pass .....	43

## SUMMARY

This study sought to investigate the interaction between two tidal inlets connected to Boca Ciega Bay. Of particular interest was the need to quantify the mechanism and magnitude of continued scour of John's Pass Inlet and to assess the stability of Blind Pass Inlet. This report summarizes the pertinent aspects of a master's thesis presented for defense by the first author on May 5, 1999.

The study consists of a field investigation, construction and calibration of a numerical hydraulic model, and analysis of predictive simulations using the calibrated model. A field survey of the Boca Ciega Bay region was conducted between April 25, 1998 and May 8, 1998. Data collected included current velocities during spring and neap tides, tide heights, and bay and inlet bathymetry. A two-dimensional, surface-water hydraulic model was constructed and calibrated to spring and neap tidal conditions. Input data included bay and inlet bathymetry, tide heights, and wind speed and direction. Model output consisted of current velocities and tide heights at 21 locations corresponding to field-survey stations. A storm-surge simulation was performed in order to predict maximum velocities at John's Pass and Blind Pass. Finally, predictive simulations were made to investigate the effects of changes in the cross-sectional area of Blind Pass and John's Pass.

Model results indicate that the average Boca Ciega Bay tidal-prism volume was

approximately 900 million cubic feet during the study period. Forty percent of this volume was fed through John's Pass and five percent through Blind Pass. Peak spring velocities were 3.6 ft/sec in the main channel at John's Pass and 2.7 ft/sec at Blind Pass.

The stability of Blind Pass and John's Pass were assessed based on: diagrams which relate cross-sectional area to maximum velocity; ratios of tidal prism to littoral drift; and relationships between cross-sectional area and tidal prism from results of the computer model. John's Pass was determined to be an inlet which will continue to scour, possibly to a cross-sectional area 60% larger than present. Blind Pass was evaluated as a depositional inlet requiring periodic maintenance dredging to remain open. Due to the relative size of Blind Pass, alterations in the area of Blind Pass do not significantly impact hydraulics at John's Pass. Changes in the cross-sectional area of John's Pass affect the tidal prism of Boca Ciega Bay as well as Blind Pass. Consequently, a more significant change in velocities at Blind Pass results.

## INTRODUCTION

Tidal inlets provide tidal conveyance from open bodies of water to more sheltered lagoons, estuaries, or bays. They are often in a state of flux due to a variety of forcing influences which control their shape and stability. The stability of an inlet describes the degree to which inlet geometry, including the cross-sectional area, location, planform, and shape is maintained with time (Bruun, 1978). Environmental factors such as tides, longshore transport, freshwater input, and wave climate influence inlet configurations (O'Brien, 1976).

### Objectives

The purpose of this report is to describe the interaction of two inlets and explore the magnitude of projected scour and deposition influencing bridge maintenance or replacement decisions for the John's Pass Bridge. The study area was Boca Ciega Bay, located along the central Gulf coast of Florida between Clearwater Harbor and the mouth of Tampa Bay. The hydraulic system consists of an approximately 16 square-mile back-barrier bay region, John's Pass, Blind Pass, and Pass-A-Grille inlets, as well as the Narrows Intracoastal Waterway (Fig. 1). The interaction of John's Pass and Blind Pass, in particular, was considered. As Blind Pass has been historically shoaling (CPE, 1992),

John's Pass has been deepening (PH&A, 1997).

The study consisted of three parts: collection of hydraulic field data in the bay and inlets; construction and calibration of a two-dimensional numerical model to simulate present flow conditions; and analysis of results of predictive simulations of the hydraulic model. More specifically, a first purpose was to evaluate hydraulic characteristics of the system at the time of investigation. The tidal prism of Boca Ciega Bay, the percentage of the prism serviced by each inlet, and the maximum current velocities at tidal passes were determined. Next, predictive scenarios representing inlet shoaling, deepening, or dredging were modeled in order to determine changes in maximum velocities and tidal-prism distribution. Finally, the stability of inlets was evaluated using empirical relationships between tidal prism and cross-sectional area (Jarrett, 1976), ratios of tidal prism to littoral drift (Bruun, 1978), and relationships between maximum velocity and cross-sectional area (O'Brien and Dean, 1972).

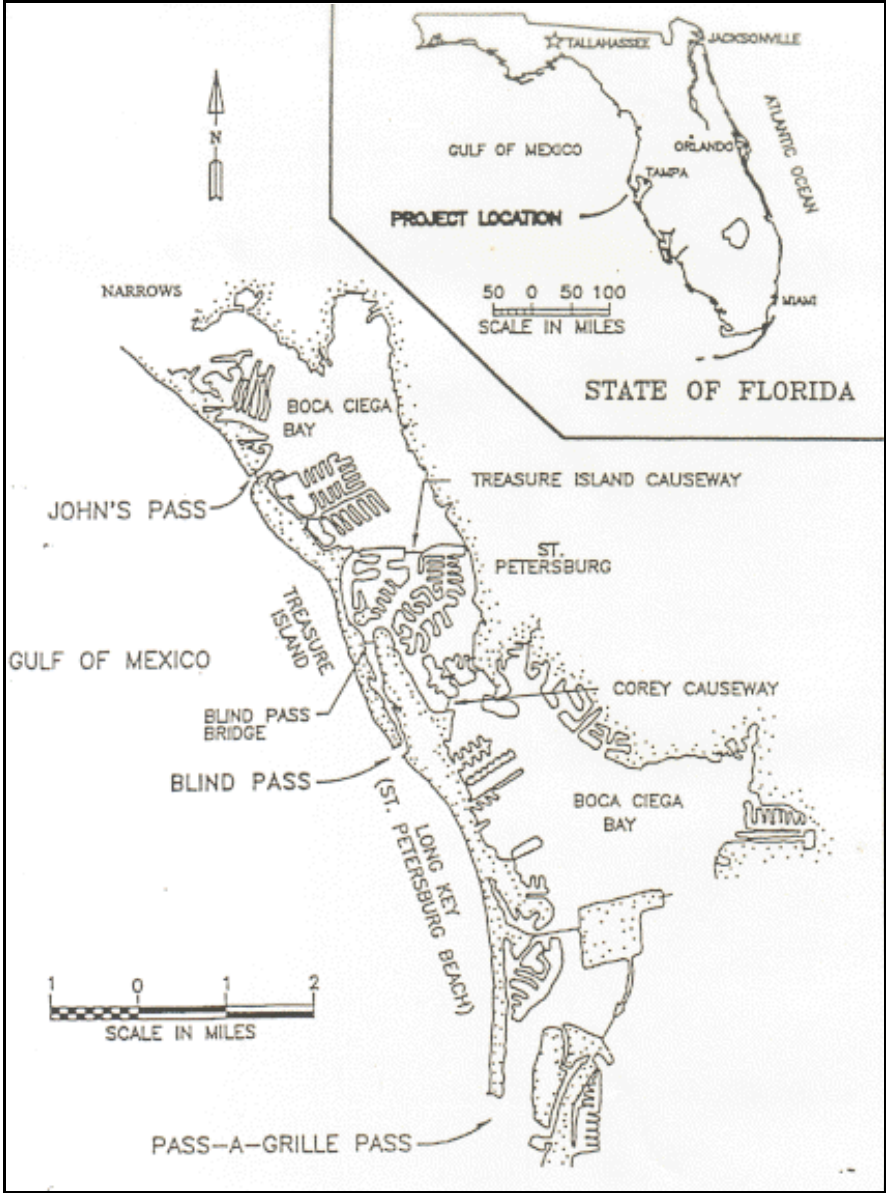


Figure 1. Boca Ciega Bay study area.

## Study Area

The central Gulf coast of Florida is characterized by a chain of barrier islands separated by tidal inlets. The region represents a low-energy, microtidal environment with semi-diurnal, mixed tides (Davis and Gibeaut, 1990). Beach and bottom sediments consist mostly of fine to very fine quartz sand. The coast may be characterized as a littoral-drift shore. Shoreline configurations are influenced largely by the distribution of sediment as well as tidal and wave action (Bruun, 1978).

The Boca Ciega Bay region includes inlets with distinct differences in size and flow characteristics. Blind Pass is a wave-dominated pass (Davis and Gibeaut, 1990). The action of wave-induced, littoral-drift transport significantly influences the inlet's configuration. As a result of sand deposition, the updrift side of Blind Pass extends seaward and in front of its downdrift shoreline (Bruun, 1978). Because of a historical reduction in tidal flow that caused sediment deposits to migrate toward shore, the inlet has no substantial ebb-tidal shoal (CPE, 1992).

John's Pass, in contrast, is a tide-dominated inlet. It has a well-defined channel and carries a sizeable tidal prism (Davis and Gibeaut, 1990). An extensive, lobe-shaped outer shoal, created largely as a result of sediment deposition by ebb-tidal currents, extends approximately 5400 feet offshore (CTC, 1993).

Hydraulic characteristics of Blind Pass and John's Pass have been affected by: changes in the configuration of Boca Ciega Bay; dredging and development activities at the individual inlets; and changes in the size of adjacent passes. The co-dependency of Blind Pass and John's Pass has been reflected in the history of their cross-sectional areas (Fig. 2). While Blind Pass has historically been closing due to shoaling, John's Pass has

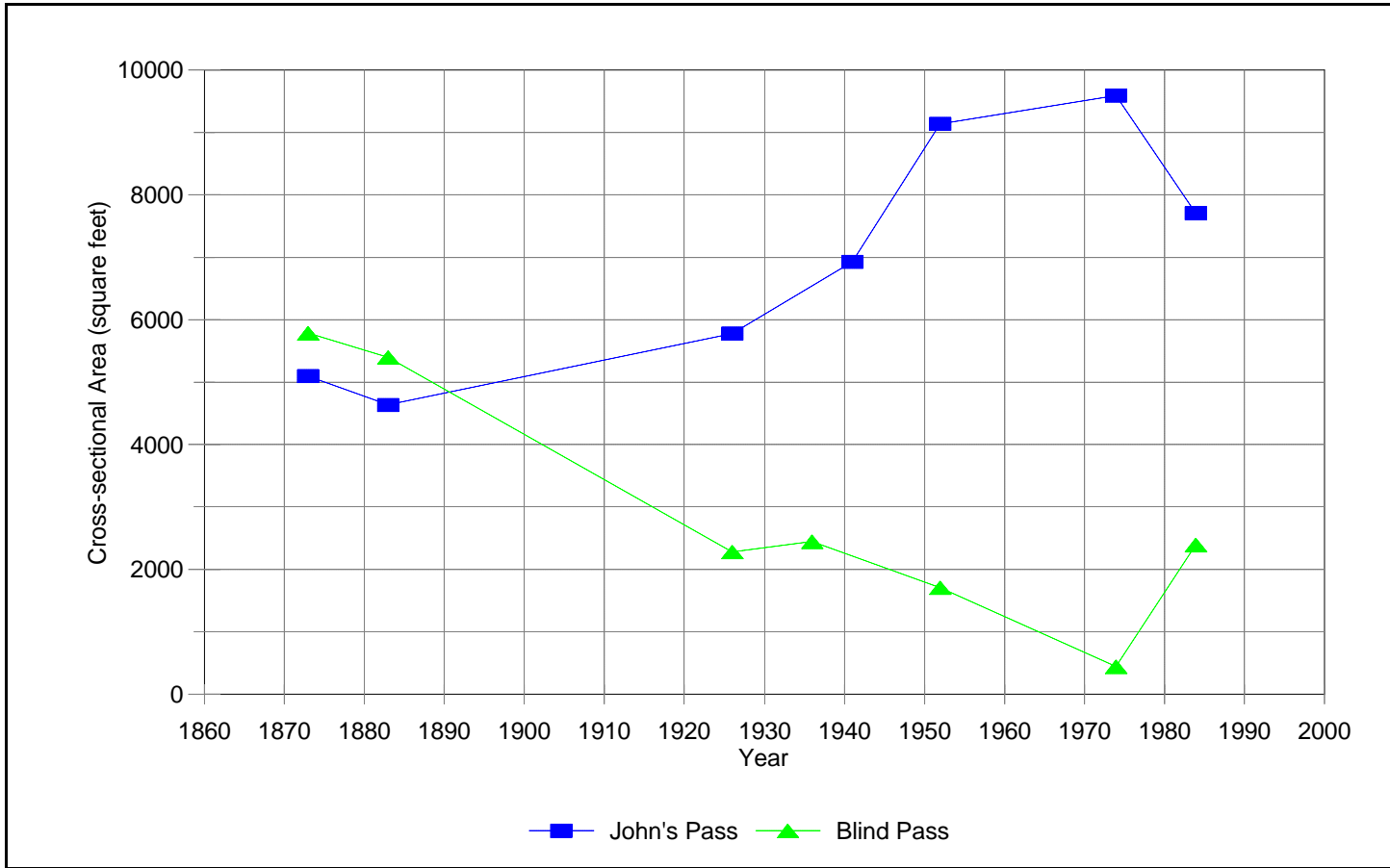


Figure 2. History of cross-sectional areas of John's Pass and Blind Pass (adapted from CPE, 1992).

been increasing in size (CPE, 1992). As a result, severe bed erosion has occurred at John's Pass (Vincent, 1992).

Dredging or development at one inlet can affect flow conditions throughout the bay. In analysis of inlet stability, factors affecting not only the individual inlet, but the hydraulic system as a whole, must be considered.

## BACKGROUND

### Evolution of Boca Ciega Bay

Although the general configuration of Boca Ciega Bay has not significantly changed since the 1970's (NOAA, 1977, 1997), an earlier history of human activity and natural events has helped the system develop its present morphologic and hydraulic characteristics. In the late 1800's, when nautical charts of Boca Ciega Bay were first published by the United States Department of Commerce Coast and Geodetic Survey (USCGS), the bay was in a natural and quite dynamic condition. During this period, Blind Pass was a mixed-energy inlet (Davis and Gibeaut, 1990). Its cross-sectional area was approximately 5800 square feet, slightly larger than John's Pass. Both inlets had a tendency to migrate toward the south (Mehta et al., 1976). Although several inlets linked the Gulf and bay, three of these passes -- Indian Pass at the Narrows (Fig. 1) and two relatively unstable openings between John's Pass and Blind Pass -- were closed by the 1930's and have remained closed. In 1916, sand was pumped into the inlet just north of Blind Pass, but the action of storm events opened and closed it again several times until 1935, when it permanently closed. By the end of the 1920's, the United States Army Corps of Engineers filled Indian Pass to help prevent further shoaling of the Intracoastal Waterway at the Narrows (Mehta et al., 1976).

By the 1920's, the original bridges across John's Pass and Blind Pass were

constructed, and they altered the natural condition of the inlets for the first time (CTC, 1993). In the following decades, development continued to impact inlet and bay hydraulics; for example, the causeway connecting mainland Pinellas County to Treasure Island was constructed from 1935 through 1937. Dredge-and-fill islands south of the causeway followed. As a result, the tidal prism through Blind Pass was substantially reduced and, it is believed, was primarily captured by John's Pass (CPE, 1992). Resultant lower current velocities at Blind Pass may be linked to that development and to an increase in channel length between 1873 and 1939 (Mehta et al., 1976). These lower velocities resulted in shoaling at Blind Pass and a reduction in its cross-sectional area (Mehta et al., 1976).

During the 1940's and 1950's, extensive dredge-and-fill operations continued throughout much of Boca Ciega Bay (CTC, 1993). As the cross-sectional area of Blind Pass decreased during this period, the size of John's Pass increased. This trend continued through the 1970's. In 1974, the area of John's Pass had reached 9500 square feet at the throat, nearly twenty times that of Blind Pass. The combined area of the two passes at this time was approximately the same as it was in the 1870's (Mehta et al., 1976).

After the completion of dredge-and-fill development and the construction of the Pinellas Bayway, the surface-area configuration of Boca Ciega Bay, broadly viewed, had been relatively well established (NOAA, 1977, 1997). Although hydraulic characteristics of John's Pass and Blind Pass are linked to the surface area of Boca Ciega Bay (CPE, 1992), the effects of local and federal dredging projects and beach nourishment efforts as well as the position of jetties, seawalls, and bridges contribute to the physical characteristics and flow regime of the two apparently co-dependent inlets (CPE, 1992).

## John's Pass

John's Pass is approximately 2100 feet long and 600 feet wide (Vincent, 1992). A tide-dominated inlet, it has extensive ebb- and flood-tidal deltas (Davis and Gibeaut, 1990) and a federally maintained navigation channel. Much of the inlet's shoreline has been hardened by seawalls. A 900-foot revetment helps stabilize the southern channel, and a fully impounded, 460-foot terminal groin extends along its northern shoreline. Only the southwest shoreline tip remains unhardened (CTC, 1993).

As a result of historical increases in tidal prism and cross-sectional area, bed erosion has occurred at John's Pass. Beginning in 1976, severe scour near bridge pilings had been noted. Several years later, three bridge pilings had become exposed while those remaining were within a few feet of exposure (Vincent, 1992). Although crutch bents, which extend into the bed of the channel, were added in 1981 to help support the bridge, continued channel lowering led to "scour critical" conditions (PH&A, 1997). Dredging operations, beach nourishment projects, construction of coastal structures, and storm events have influenced the flow regime of John's Pass and the configuration of adjacent shorelines throughout the history of this pass (Table 1).

Table 1  
History of John's Pass

- 1848: A major hurricane cut through the Boca Ciega barrier island to create John's Pass (CTC, 1993).
- circa 1924: Indian Pass was closed by the Army Corps of Engineers to prevent shoaling at the Narrows (Mehta et al., 1976). Its closure appears to have contributed to an increase in the size of John's Pass (Vincent, 1992).
- 1926: The original bridge across John's Pass was built.
- 1957: Thirty-seven groins were placed along Madeira Beach (CTC, 1993). After the construction of these coastal structures as well as a jetty at the inlet's northwest shore in 1961, a historical erosional trend along the shoreline north of John's Pass reversed to one of accretion (PH&A, 1997).
- 1960: Dredged material from John's Pass was deposited approximately 20,000 feet offshore (Mehta et al., 1976). This material as well as sediment dredged from the inlet in 1966 would in subsequent years migrate onshore and attach to the coastline south of John's Pass to create what became known as O'Brien's Lagoon (CTC, 1993). Recession of the beach south of the inlet between 1974 and 1992 appears to have been related to the artificial filling of the lagoon in 1971 and subsequent erosion of the material (CTC, 1993).
- 1961: A 460-foot jetty was constructed at the northwest corner of John's Pass (CTC, 1993).
- 1966: John's Pass was dredged as part of a federal navigation project. In addition, a 920-foot revetment was constructed along the inlet's southern shore (CTC, 1993).  
Net littoral drift along the coast near John's Pass was toward the south (Vincent, 1992); in response to the hardening of its northern and southern shorelines, the inlet's thalweg migrated to the south side of the pass (PH&A, 1997).
- 1971: The original bridge across John's Pass was removed (Vincent, 1992), and a new one was constructed west of the original (Christensen and Langley, 1975).
- 1987: The jetty and revetment on the inlet's northern shore were rehabilitated (CTC, 1993).

## Blind Pass

Blind Pass, approximately 500 feet wide at its entrance (FDC, 1997), separates Treasure Island from Long Key. The evolution of this inlet has been strongly influenced by human activity (Table 2). In 1937, a jetty was built on the south side of the inlet to prevent migration of the pass. This structure was lengthened in the 1950's and again in the 1970's. It now extends to a distance of approximately 260 feet perpendicular to the shore. In addition, a 315-foot breakwater, angled toward the south, was also added in 1986 (CPE, 1992).

A 425-foot jetty was constructed on the northern shore of Blind Pass in 1962. The jetty was extended and raised in the 1970's, and, in the 1980's, it was lengthened to reach a distance of 520 feet into the Gulf (CPE, 1992).

A mixed-energy inlet in the late 1800's, Blind Pass has been shoaling throughout much of its known history. It is now classified as wave-dominated (Davis and Gibeaut, 1990). The decrease in throat area has been linked to the building of Treasure Island Causeway as well as to dredge-and-fill operations; the construction of Paradise Island at the bay side of the channel is believed to have restricted flow (Mehta et al., 1976). Consequently, the cross-sectional area of Blind Pass decreased from 2,450 square feet to 442 square feet following dredge-and-fill development. More recent changes in the size of Blind Pass are a result of periodic dredging and shoaling of the inlet's channel (CPE, 1992).

Table 2  
History of Blind Pass

- 1873: Blind Pass was located approximately one mile north of its present location. An alternate entrance existed north of the inlet (Loeb, 1994).
- 1926: The original bridge over Blind Pass was built.
- 1935: The alternate entrance to Blind Pass was closed and has remained closed (Loeb, 1994).
- 1937: A jetty was built on the south side of Blind Pass to halt migration of the pass. The jetty was extended to a length of 261 feet in the 1970's, and a 315-foot breakwater, angled toward the south, was added in 1986 (CPE, 1992). In addition, a channel through shoals north of the jetty was dredged (Mehta, et al., 1976).
- 1962: A 425-foot jetty was constructed along the northern shore of Blind Pass (Mehta et al., 1976). A groin was added along the northern shore in 1976 and was extended to a length of 520 feet in 1983 (CPE, 1992).
- 1963: Blind Pass was dredged, and fill was used as beach nourishment north of the inlet. In addition, the inlet was used as a source of sand for adjacent beaches in 1969, 1975, 1979, 1983 and 1990 (CPE, 1992).
- 1997: The current bridge across Blind Pass was built.

## Methods Used to Evaluate the Stability of John's Pass and Blind Pass

Tidal prism, the amount of water which flows through an inlet during a flood or ebb tide, is the primary factor characterizing flow conditions across an inlet section. In addition, tidal inlets on a littoral drift shore are influenced by a combination of waves, winds, and longshore currents (O'Brien, 1976).

### *Empirical Relationships*

Jarrett's (1976) regression analysis was used to evaluate the relationship between tidal prism and cross-sectional area of John's Pass and Blind Pass. According to results of Jarrett's (1976) study, the relationship between tidal prism and cross-sectional area may be described by power functions in the form:

$$A = CP^n, \quad (1)$$

where  $A$  = cross-sectional area ( $\text{ft}^2$ ),  $P$  = spring or diurnal tidal prism ( $\text{ft}^3$ ), and  $C$  and  $n$  are regression constants which then could vary with local conditions. Jarrett (1976) developed the following equation to describe the relationship between tidal prism and cross-sectional area for Gulf coast inlets:

$$\text{for all inlets, } A = 5.02 \times 10^{-4} P^{0.84}, \quad (2)$$

In order to assess the stability of John's Pass and Blind Pass, results of the calibrated model were to used to determine the relationship between the tidal prism and the cross-sectional area of each inlet.

### *Ratios of Tidal Prism to Littoral Drift*

The ratio of tidal prism, P, to annual littoral-drift quantities, M, was used to describe the relative stability of each tidal pass. Inlets may be characterized as poor, fair to poor, or good in stability based on such ratios (see Table 3).

Table 3  
Stability index proposed by Bruun (1978)

P/M	Stability Rating	Inlet Characteristics
>150	Good	Relatively few bars, well flushed channels
$100 < P/M < 150$	Fair	More prominent offshore bar formation
0		
$50 < P/M < 100$	Fair to Poor	Large offshore bar, often with a channel through it
<50	Poor	Unpredictable channels, unstable openings

### *Stability Diagrams*

Stability diagrams which depict the relationship between the cross-sectional area and maximum velocity at John's Pass and Blind Pass were constructed from results of predictive simulations of the numerical model. A "critical" gorge area (Fig. 3), associated with a maximum velocity, may be used to distinguish stable from unstable conditions (O'Brien and Dean, 1972). In a stable situation, for example, a decrease in cross-sectional area due to sediment deposition causes an increase in velocity because currents

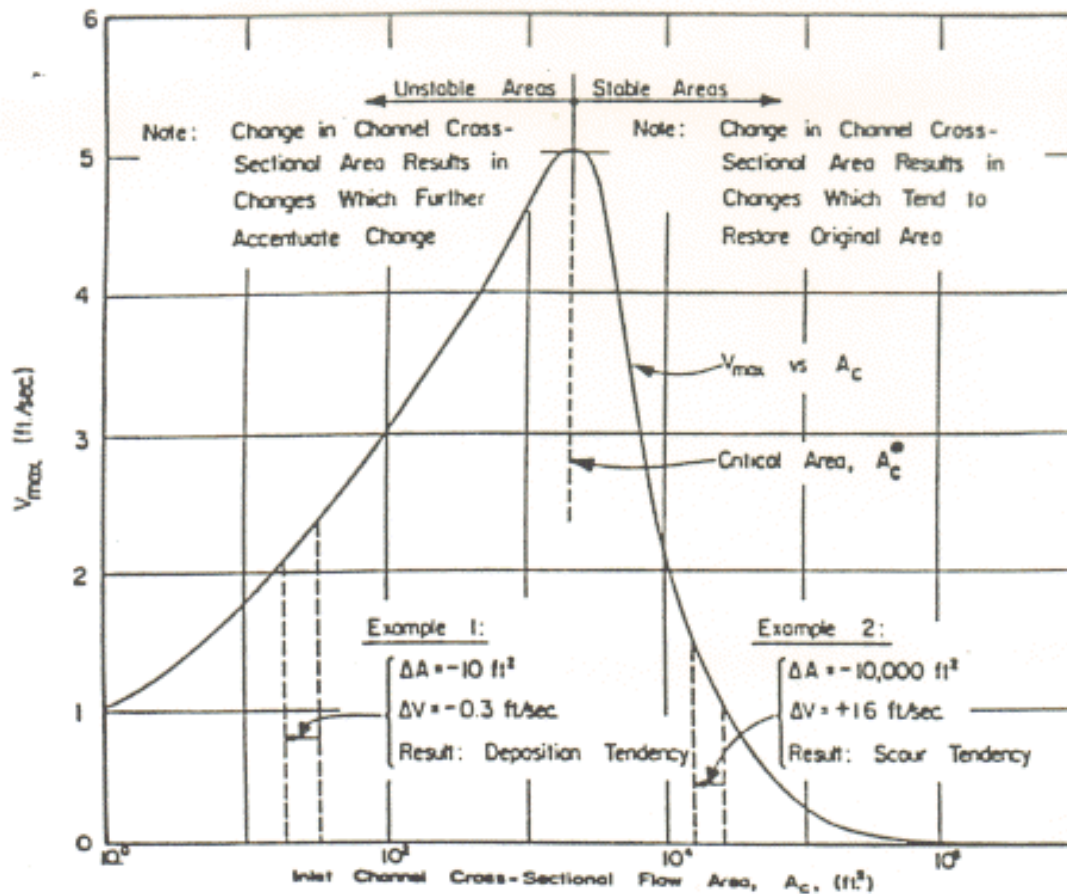


Figure 3. Escoffier's stability concept (after O'Brien and Dean, 1972).

## CONSTRUCTION OF THE NUMERICAL MODEL

A two-dimensional, numerical hydraulic model was used to simulate flow through Boca Ciega Bay, John's Pass, and Blind Pass (Ross et al., 1999). The work consisted of two parts: 1. collection of field data in Boca Ciega Bay, Blind Pass, and John's Pass; and 2. construction and calibration of the model.

### Field Study

A field survey of the study area was conducted between April 25, 1998 and May 8, 1998. The period included both spring- and neap-tide conditions. Data collected during the study included tidal heights at four locations along the boundary of the model domain, velocities at 21 stations throughout the bay and inlets, and bathymetry at various locations within the study area.

*Tidal Heights.* Stilling-well tide gauges were installed on April 25, 1998 in the vicinity of John's Pass, Pass-A-Grille inlet, Indian Key southwest of Maximo Point, and at the Narrows Intracoastal Waterway. Tidal heights were recorded at 10-minute intervals. Gauges remained in place through May 8, 1998. The location of each of the four gauges is shown in Figure 4.

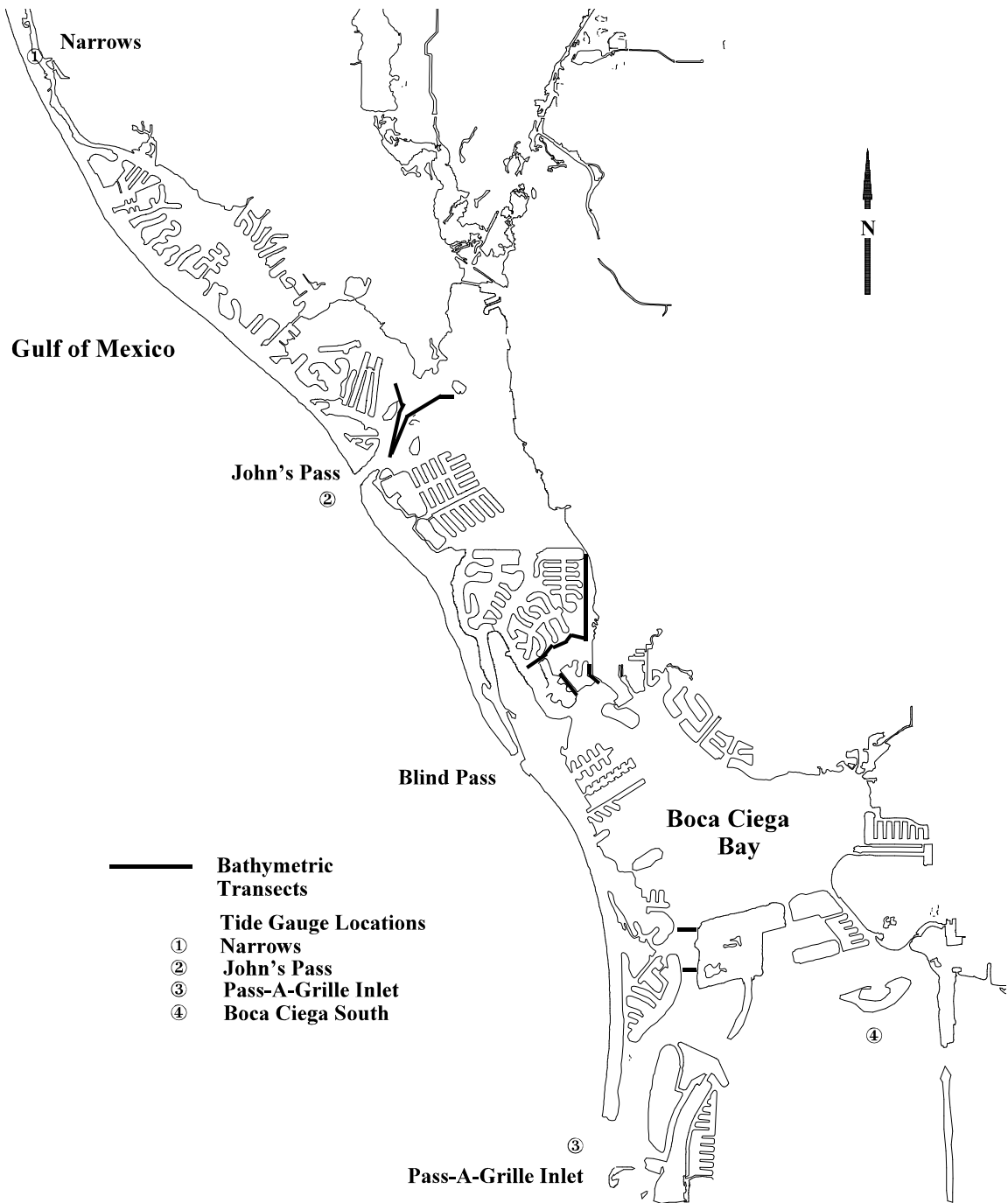


Figure 4. Location of tide gauges and bathymetric transects in the Boca Ciega Bay study area.

*Velocities.* The 21 velocity stations were at bridge locations throughout Boca Ciega Bay, including at John's Pass, Blind Pass, and the Narrows Intracoastal Waterway (Figure 5). Data were collected during two periods, April 28-29, 1998 and May 6-7, 1998, for spring- and neap-tide conditions, respectively.

Current speeds and directions were measured on the upstream sides of main channels. Velocities were measured at depths of 0.6 times the water depth at relatively deep channels and at 0.8 and 0.2 times the water depth at shallower channels. Current speeds and directions at John's Pass were measured at locations along the lateral extent of the cross section.

*Bathymetric Transects.* A recording fathometer was used to determine depths throughout the study area. Fathometer traces were recorded at bridge locations and at areas shown in Figure 4.

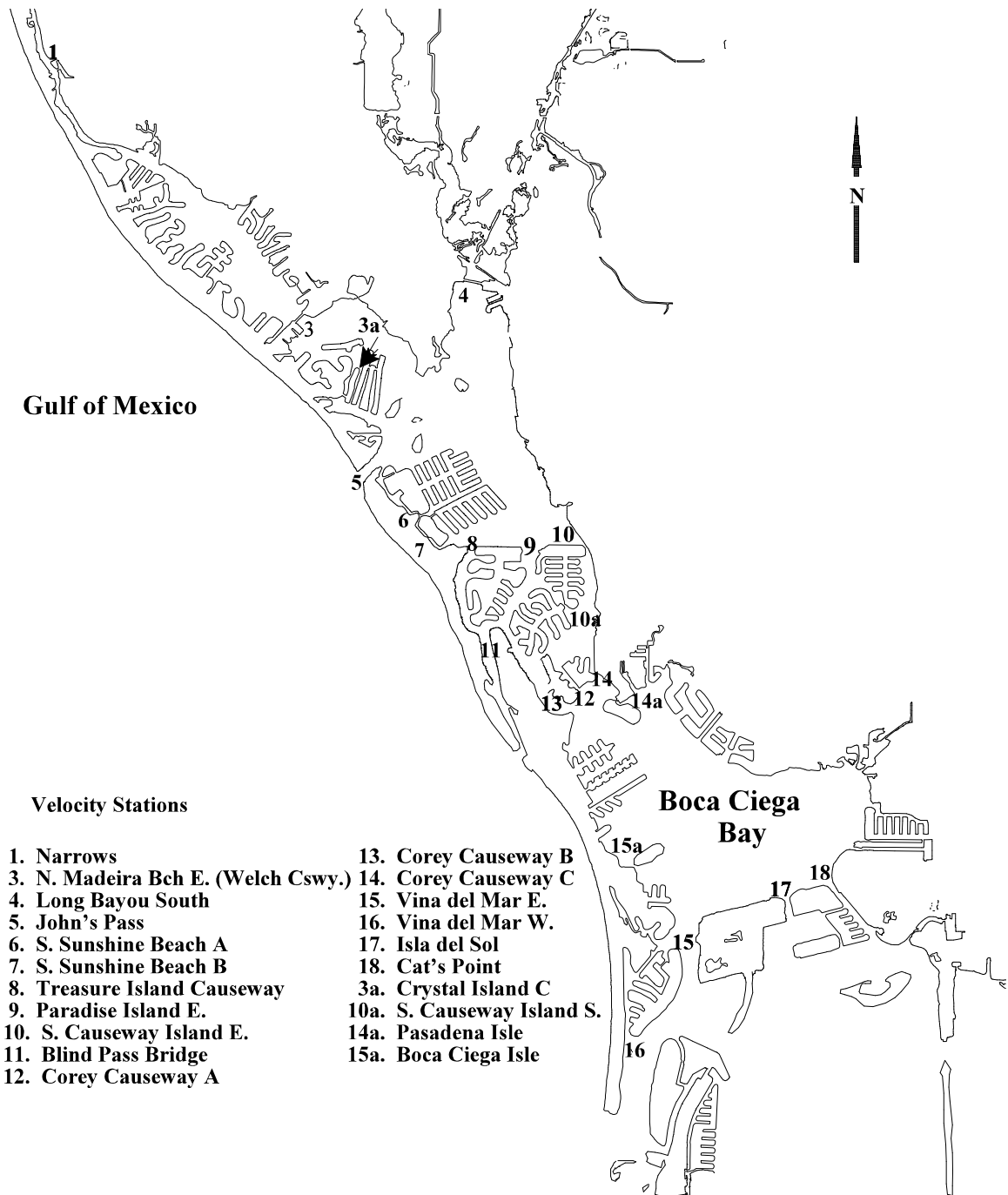


Figure 5. Location of velocity stations in the Boca Ciega Bay study area.

## Computer Model

A two-dimensional hydraulic model was used to simulate flow throughout Boca Ciega Bay, Blind Pass, and John's Pass. The model uses the vertically-integrated equations of motion and continuity to solve for depth-integrated transports and water-level heights (Ross et al., 1999). Results are calculated using an explicit finite-differencing method. Detailed descriptions of terms in the equations of motion and continuity, numerical methods of solution, and components of the data sets required for model simulation can be found in the USF-CMHAS Hydraulic and Water Quality Model (HYDQUAL) Documentation (Ross et al., 1999).

*Construction of the Boca Ciega Bay Model.* Geographic and hydraulic characteristics of the bay and inlets were determined in order to develop a model of the Boca Ciega Bay region. First, a grid array consisting of 45 rows and 105 columns was constructed (Figure 6). Each grid cell represents a distance of 600 feet in length and 600 feet in width. Next, hydraulic data sets were assembled. The latitude and longitude of the origin of the study domain, bay and inlet bathymetry, hourly measured winds, and measured tidal heights were included in the input data set. Bottom elevations of the study region were determined from: USACOE (1998, 1997) surveys of John's Pass and the Intracoastal Waterway; NOAA (1995) navigation charts; a hydrographic survey of Blind Pass (FDC, 1997); and data obtained during the field study. Wind speed and direction measurements at Azalea Park were obtained from the Pinellas County Department of Environmental Management, Air Quality Division. Tidal heights, measured during the field survey, were used to drive the model.

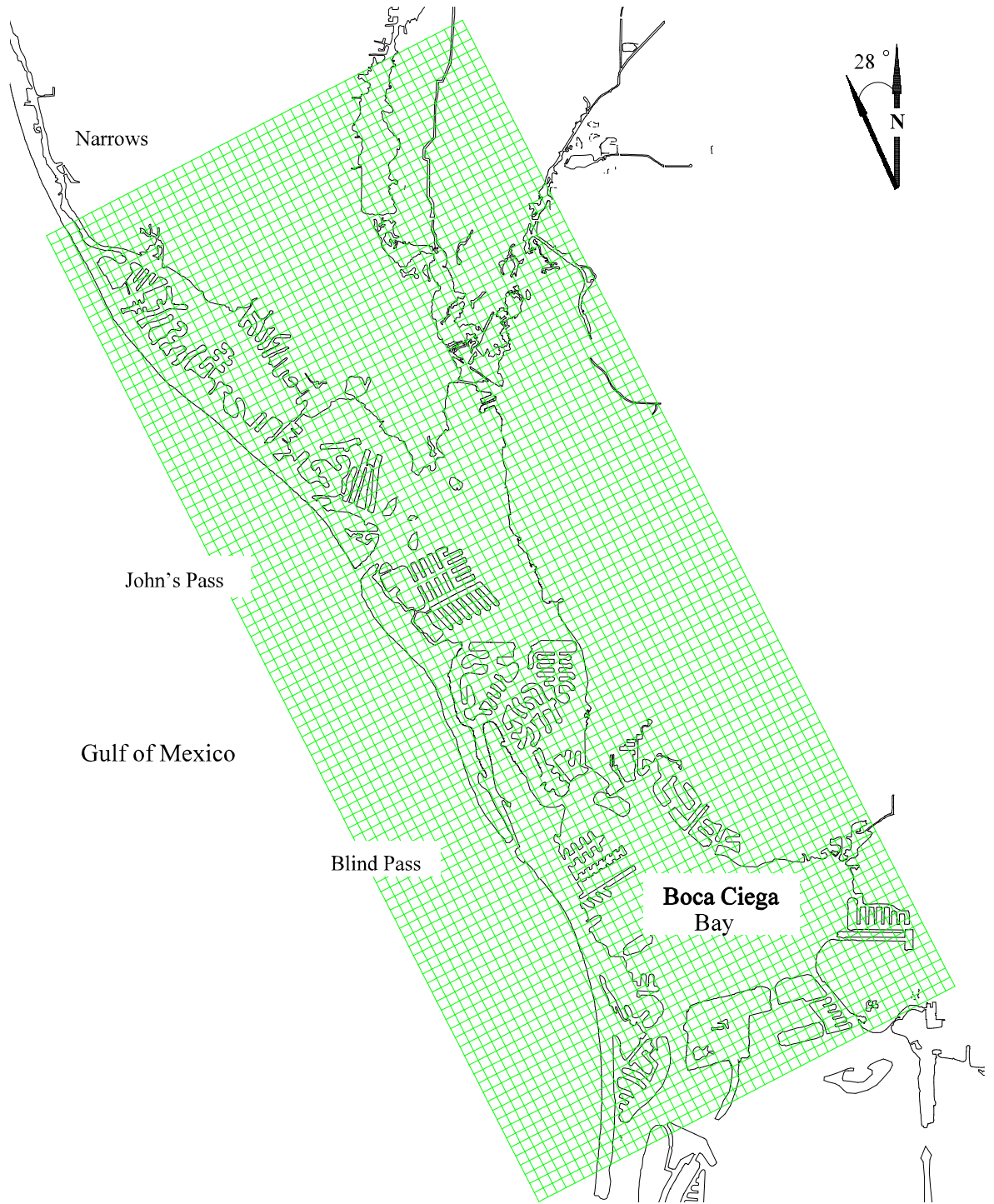


Figure 6. Grid array of the Boca Ciega Bay model.

Sub-grid features, referred to as “gates,” were designated in the data set in order to represent shoals, obstructions to flow, or constricted channels (Ross et al., 1999). Each “gate” represents a cell side and consists of a main channel, a secondary channel, and a barrier (obstructed) section. Values for depths and widths for each channel (Appendix A) were assigned based on fathometer traces and hydrographic surveys of the study region.

*Boca Ciega Bay Model Calibration.* The Boca Ciega Bay model was calibrated for the two measurement periods. Output included velocities and tidal heights corresponding to the 21 velocity stations. The measured velocities were used for calibration. Output was reported in 15-minute intervals. The model was run for 72 hours of simulation for spring- and neap-tide periods. The initial 24 hours were used to remove transients, which represent inaccurate output as a result of incorrect startup values in the model solution. Velocities and tidal heights from the final 48 hours of simulation were used for calibration.

*Tides.* Measured tidal heights at the Pass-A-Grille inlet tide station were used as the driving function of the model. Leads, lags, and amplitude adjustments for tides at each open-water segment were then calculated relative to the Pass-A-Grille inlet tide function. The assigned values are listed in Appendix A.

*Additional Constrictions.* Additional “gates” were added to the model to depict, in detail, the location of shoals, constricted channels, or obstructions to flow. The cross section of John’s Pass consisted of five cell faces which represented the inlet channel and adjacent

bottom topography. Depths at the throat section were determined from bathymetric transects recorded during the field study. Bathymetry in regions adjacent to the inlet were obtained from an USACOE (1998) survey of John's Pass. Similarly, nine gates were defined at the entrance of Blind Pass. Bathymetric data collected during the field study and a hydrographic survey of Blind Pass (FDC, 1997) were used to determine the dimensions of the inlet's cross section. Details of channel widths and depths of each defined cell face are in Appendix A.

#### *Flow Simulation of Boca Ciega Bay*

The calibrated model was used to simulate flow for the 11-day period, representing conditions between April 27, 1998 and May 7, 1998. The first four days of the simulation corresponded to spring tidal ranges; the last three days represented neap conditions.

#### *Storm Surge Simulation of Boca Ciega Bay*

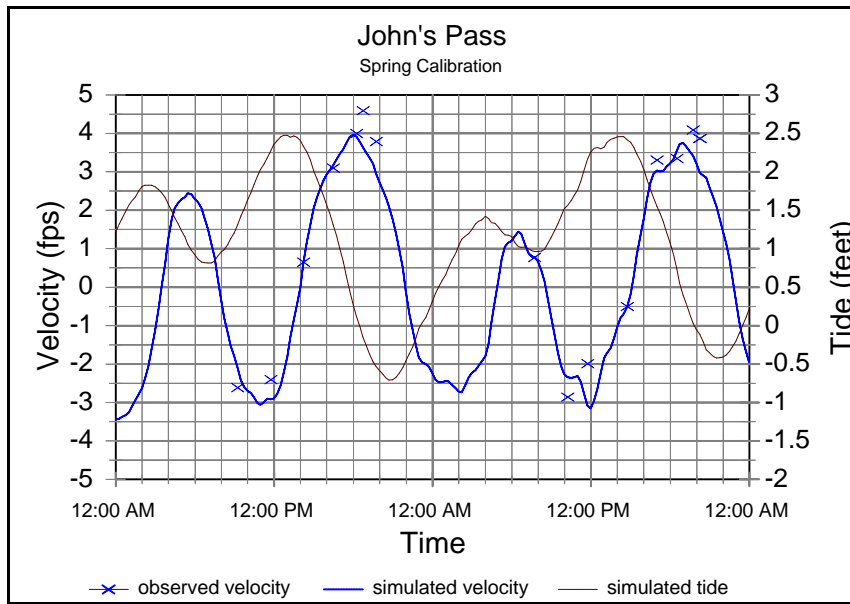
A 100-year storm surge simulation was performed for a 35-hour simulation period. Tidal heights were obtained from the Florida Department of Environmental Protection Pinellas County Storm Surge Model Study (Dean et al., 1995). Time lags were set to 0 minutes at each open-water segment. Wind speeds reached a maximum of 65 knots; wind directions represented extreme conditions. Land elevations were generated from a triangular irregular network (TIN) of the USGS 5 foot contour digital line graph (DLG). These elevations were included in order to simulate barrier island overtopping scenarios and more appropriately account for increased tidal prism of landward flooded cells.

## RESULTS OF CALIBRATION

The velocities and tidal heights at John's Pass and Blind Pass resulting from the calibrated model are shown in Figures 7 and 8. Model output at the remaining data-collection stations are illustrated in Appendices B and C.

Results determined from output of the 11-day simulation were: peak flood and ebb velocities at John's Pass and Blind Pass; discharge through each inlet and through channels along the boundary of the model domain; tidal prism of Boca Ciega Bay and the percentage carried by each inlet and boundary channel; and net flow directions through each inlet and boundary channel.

(a)



(b)

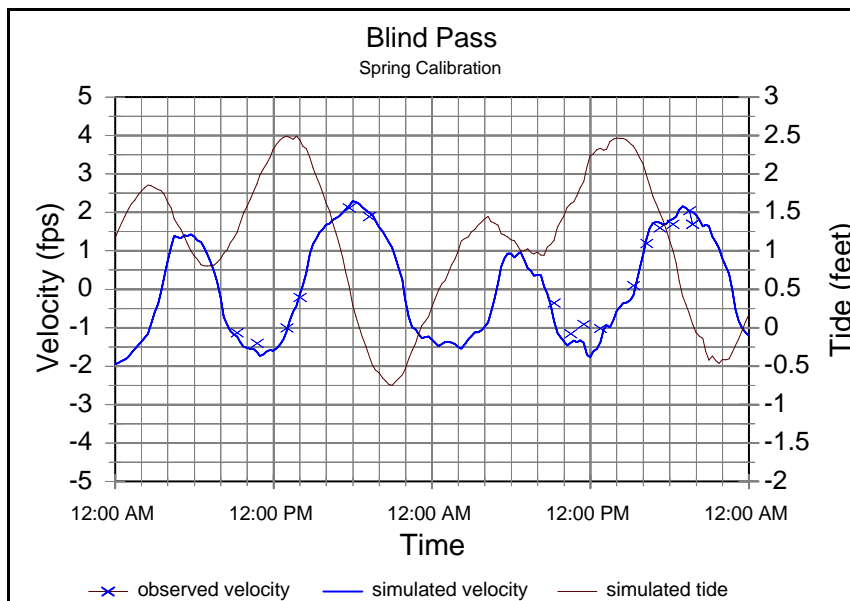
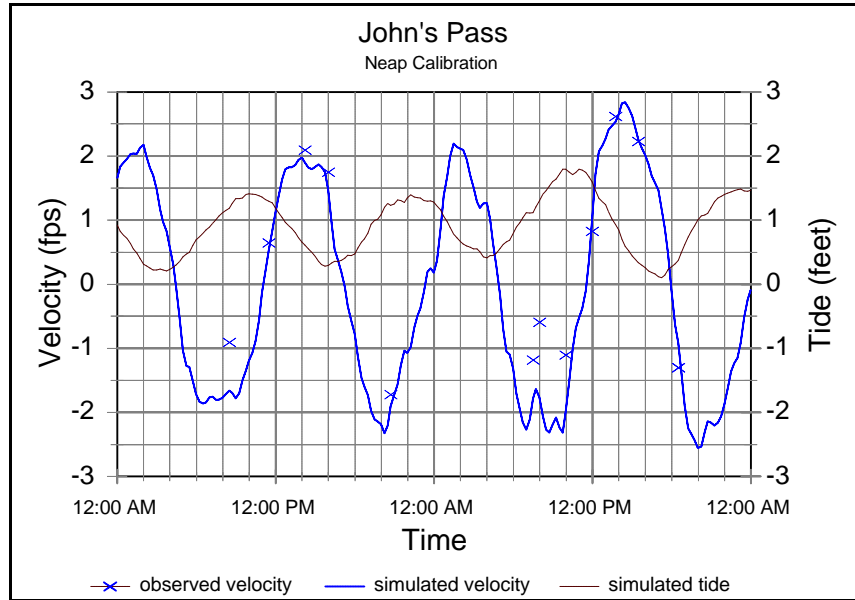


Figure 7. Results of spring-tide model calibration at (a) John's Pass and (b) Blind Pass.

(a)



(b)

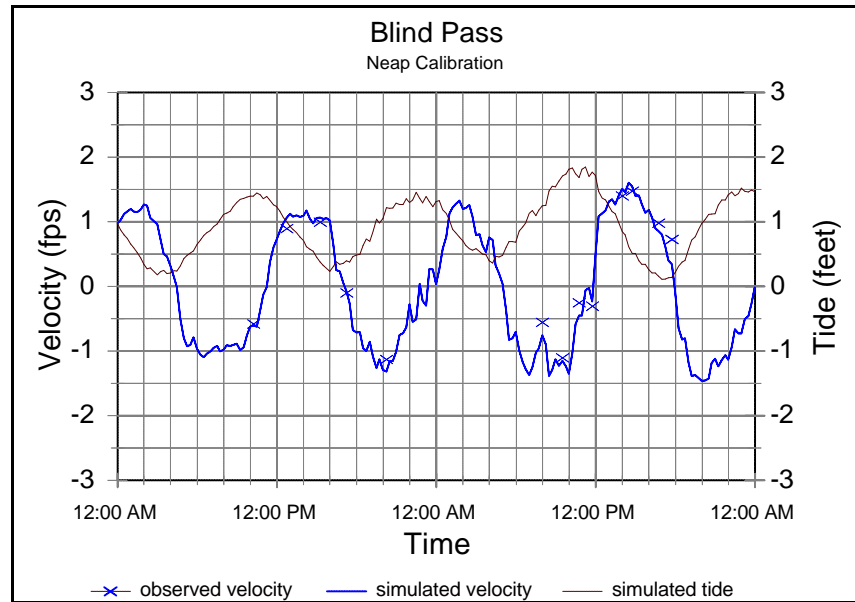


Figure 8. Results of neap-tide model calibration at (a) John's Pass and (b) Blind Pass.

## Peak Velocities

Simulated velocities in the main and marginal channels at John's Pass and Blind Pass are in Appendix D. Maximum flood and ebb velocities obtained by averaging peak velocities during four days of spring tides (principally diurnal) and three days of neap tides (including semi-diurnal) are in Table 4:

Table 4  
Peak channel velocities at Johns' Pass and Blind Pass

Inlet Channel	Peak Spring Velocity (ft/sec)		Peak Neap Velocity (ft/sec)	
	Flood	Ebb	Flood	Ebb
John's Pass (Main)	3.3	3.9	2.3	2.6
John's Pass (Secondary)	3.1	3.5	2.1	2.4
Blind Pass (Main)	2.4	2.9	1.6	1.8
Blind Pass (Secondary)	0.8	0.9	0.6	0.7

## Discharge and Cumulative Volumes

Discharge ( $\text{ft}^3/\text{sec}$ ) across the throat cross section of each channel was calculated according to the fundamental continuity equation which relates volume, area, and velocity:

$$Q = VA, \quad (3)$$

where  $Q$  = discharge ( $\text{ft}^3/\text{sec}$ ),  $A$  = cross sectional area of the channel ( $\text{ft}^2$ ), and  $V$  = average velocity perpendicular to the section ( $\text{ft}/\text{sec}$ ) (McKiernan, 1993).

The volume of water that passes a cross section in a given amount of time may be expressed as :

$$\nabla = A \cdot v(t) \Delta t \quad (4)$$

where  $\nabla$  = volume of water (ft<sup>3</sup>), A = the cross-sectional area (ft<sup>2</sup>), v = velocity (ft/sec) across the section and t = time (sec). Flow rates calculated from equation 3 and from model output at John's Pass, Blind Pass, and Boca Ciega Bay are shown in Figures 9 and 10. Cumulative volumes computed from equation 4 and from velocities and tidal heights generated by the model are also displayed. A linear-fit regression line indicates net flow directions at each pass. Curves for the remaining channels are shown in Appendix E.

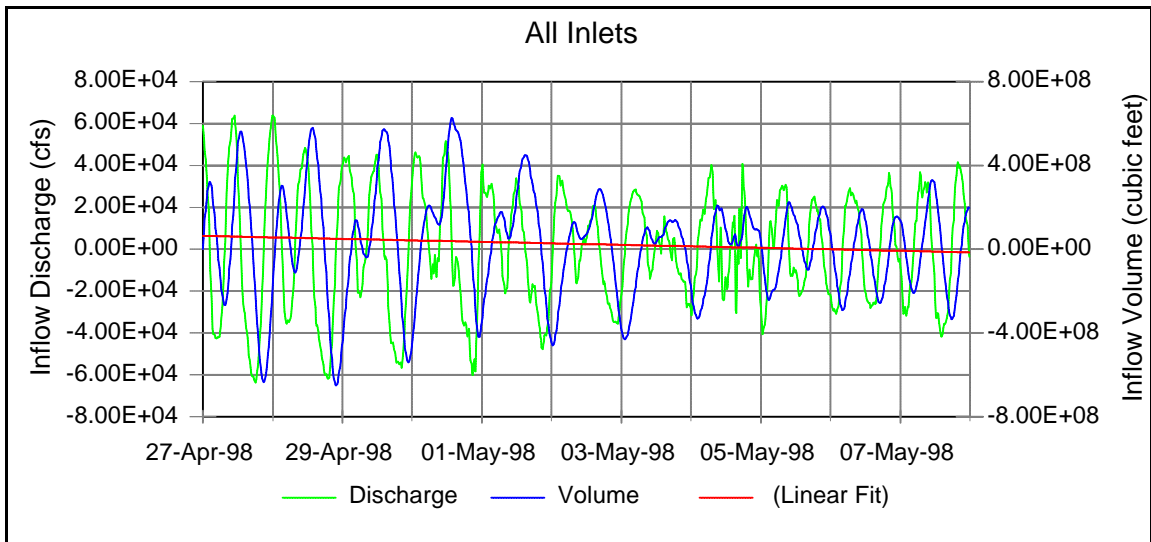
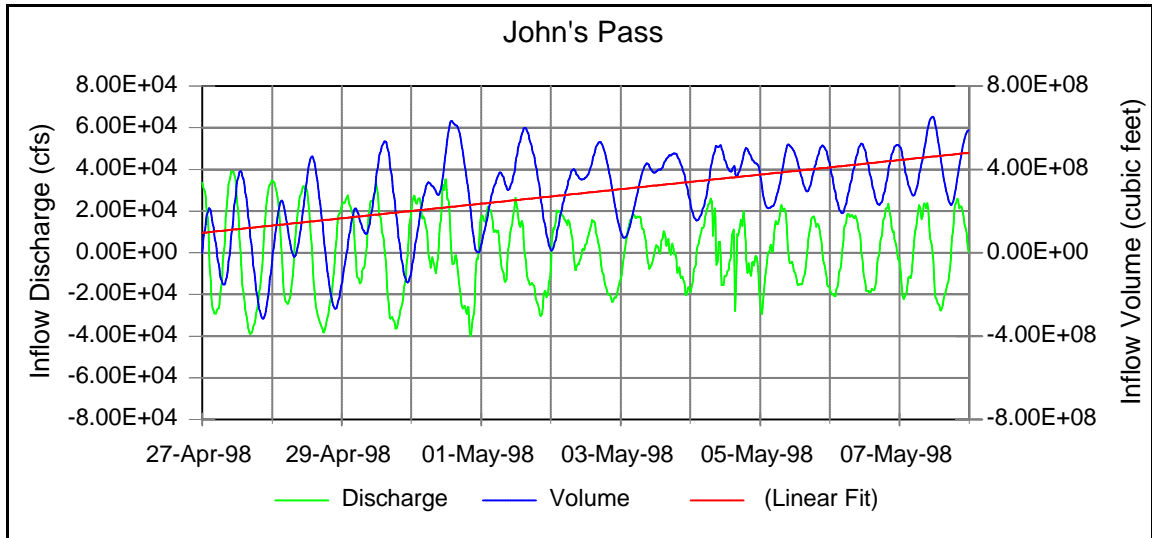


Figure 9. Discharge, volume, and net flow of Boca Ciega Bay as a result of the 11-day flow simulation.

(a)



(b)

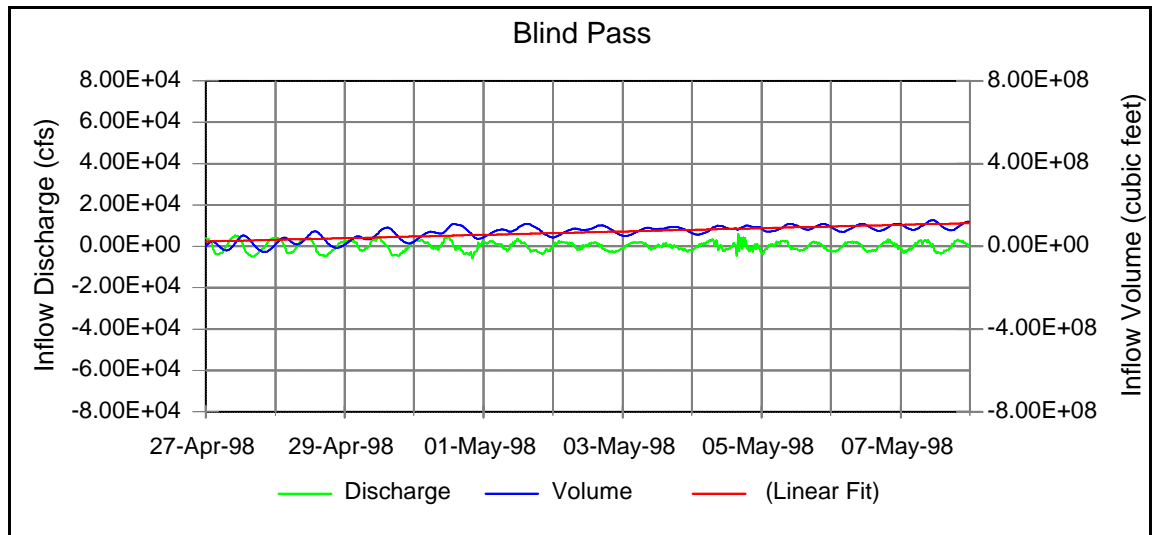


Figure 10. Discharge, volume, and net flow at (a) John's Pass and (b) Blind Pass as a result of the 11-day flow simulation.

## Net Flow

The slopes of the linear regression lines of the volume curves may be used to approximate net flow quantities and directions for the simulation period. Daily flow volumes for each channel along the boundaries of the model domain are shown in Table 5. Volumetric trends fluctuate at the Vina del Mar East and Isla del Sol channels within the 11-day period (Appendix E).

Table 5  
Net flow for 11-day simulation

Inlet or Channel	Flow Quantity (ft <sup>3</sup> /day)	Direction
John's Pass	3.49 E+07	In
Vina del Mar East	-7.10E+06	Out
Vina del Mar West	1.53E+07	In
Cat's Point	-4.78E+07	Out
Isla del Sol	-7.49+E06	Out
Blind Pass (throat)	8.08E+06	In
Narrows	-3.13E+06	Out
Boca Ciega Bay	-7.13E+06	Out

Average water-level elevations between day 1 and day 11 at boundary channels dropped approximately 0.1 feet, according to the model.

Tidal prism volumes are shown for spring, neap, and 11-day simulation periods (Table 6). In addition, the percentage of bay prism carried by each channel is indicated.

**Table 6**  
Tidal prism of channels serving Boca Ciega Bay

Inlet or Channel	11-Day Avg. Prism (ft <sup>3</sup> )	% of Bay	Avg. Spring <sup>1</sup> Prism (ft <sup>3</sup> )	% of Bay	Max. Spring Prism (ft <sup>3</sup> )	% of Bay	Avg. Neap Prism (ft <sup>3</sup> )	% of Bay
John's Pass	3.5E+08	40	7.0E+08	40	7.3E+08	37	3.1E+08	39
Vina del Mar E.	2.7E+08	30	5.5E+08	31	6.5E+08	33	2.4E+08	30
Vina del Mar W.	3.1E+07	3	6.1E+07	4	6.2E+07	3	2.6E+07	3
Cat's Point	1.2E+08	13	2.0E+08	11	2.5E+08	12	1.1E+08	13
Isla del Sol	6.5E+07	7	1.2E+08	7	1.7E+08	9	5.9E+07	8
Blind Pass (throat)	4.3E+07	5	7.9E+07	5	8.1E+07	4	3.7E+07	5
Narrows	1.7E+07	2	4.0E+07	2	4.1E+07	2	1.4E+07	2
Boca Ciega Bay	9.0E+08	100	1.7E+09	100	2.0E+09	100	7.8E+08	100

<sup>1</sup>Average of predominant diurnal tide.

#### Peak Velocities Resulting from Storm-surge Simulation

Peak velocities at John's Pass resulting from the 100-year storm surge simulation were 7.6 feet/second during the flood tide and 6.8 feet/second during the ebb tide. Peak flood and ebb velocities at Blind Pass were 3.2 feet/second.

## STABILITY OF THE PASSES

### Empirical Relationships

The cross-sectional area of Blind Pass during the study of Boca Ciega Bay was approximately 2500 square feet; the corresponding spring tidal prism was  $7.9 \times 10^7$  cubic feet. At John's Pass, the measured cross-sectional area was approximately 10,200 square feet. A spring tidal prism of  $7.0 \times 10^8$  cubic feet was determined from model data. Tidal prism versus area values plotted against results of Jarrett's (1976) original regression analysis (equation 2) are shown in Figure 11.

Plots of prism versus area for John's Pass and Blind Pass show that values for each of the inlets lie close to Jarrett's (1976) regression line (Fig. 11). This relationship, however, does not account for variability in grain-size, net longshore transport rates, or hydraulic characteristics (O'Brien, 1976), which can vary significantly from one inlet to the next. Jarrett's (1976) analysis does not distinguish between scouring and depositional inlets. Values for John's Pass and Blind Pass show little deviation from the original regression line even though hydraulic characteristics of each inlet differ significantly.

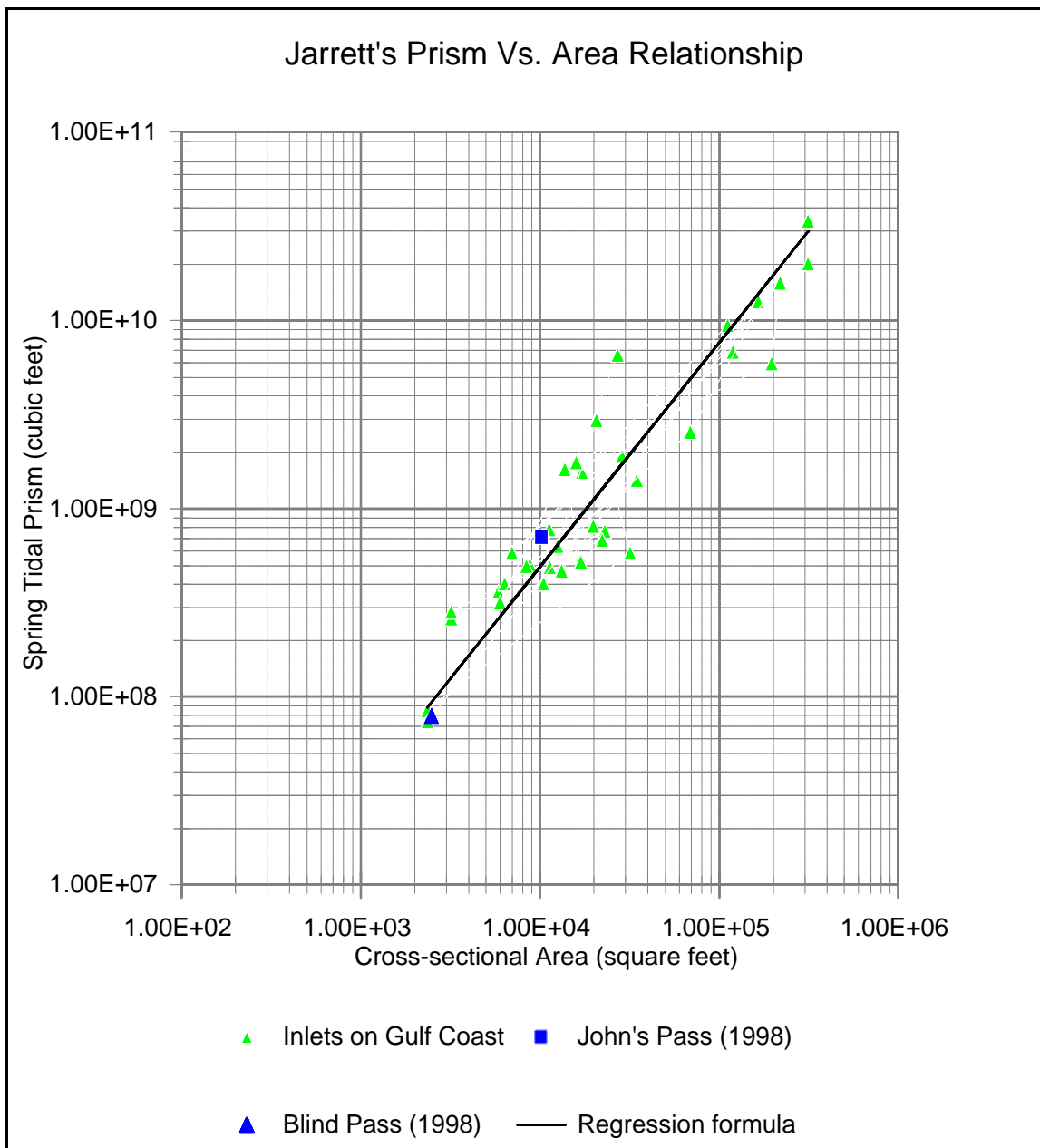


Figure 11. Jarrett's (1976) area versus prism regression analysis and tidal prism values for John's Pass and Blind Pass produced by the Boca Ciega Bay model.

## Ratios of Tidal Prism to Littoral Drift

Bruun's (1978) stability index (Table 3) characterizes inlets from the ratio of tidal prism to gross littoral-drift quantities that reach the inlet's channel. Net littoral-drift estimates for John's Pass ranged from  $8.1 \times 10^5$  to  $1.35 \times 10^6$  cubic feet per year toward the south (CTC, 1993). The spring tidal prism of John's Pass that resulted from the Boca Ciega Bay model was  $7.0 \times 10^8$  cubic feet. Based on a littoral-drift quantity of  $1.35 \times 10^6$  cubic feet per year, the ratio of tidal prism to littoral drift for the inlet is 522. An inlet with a value of greater than 150 may be classified as relatively "good" stability according to Bruun's stability index (Table 3)

The predominant direction of longshore transport at Blind Pass varies seasonally. In spring and summer, sand is primarily carried to the north, in fall and winter to the south. Longshore-transport estimates in the vicinity of Blind Pass were  $1.97 \times 10^6$  cubic feet per year toward the north and  $2.65 \times 10^6$  cubic feet per year toward the south (CPE, 1992). The spring tidal prism computed from output of the model was  $7.9 \times 10^7$  cubic feet. The ratio of tidal prism to littoral drift, based on a longshore transport average of  $2.31 \times 10^6$  cubic feet per year at the entrance of the inlet, is 34. The ability of Blind Pass to maintain a channel may be rated as "poor" (Table 3).

It should be noted that littoral-drift quantities used to assess stability at John's Pass and Blind Pass represent theoretical values obtained from shoreline orientations and wave data (CTC, 1993, CPE, 1992) and were not based on data measured at the inlets. The reliability of the method is difficult to assess. Furthermore, net littoral-drift values may be regarded as an estimate of the total amount of sediment that interacts with the inlet channel (Bruun, 1978).

## Stability Diagrams from Predictive Simulations

The tendency of John's Pass and Blind Pass to scour or deposit sediment may be characterized by relating the maximum velocity to the cross-sectional area of the inlet (Escoffier, 1940, 1977). The cross-sectional area of Blind Pass during the approximate time of the study was determined to be 2500 square feet at the throat. Maximum spring velocities in the main channel averaged 2.7 ft/sec. Peak spring velocities, weighted by area across the width of the cross section, averaged 1.8 ft/sec. Results of successive computer runs in which the main and marginal channel depths at the Blind Pass throat section were increased and then decreased in 10-percent increments produced maximum spring velocities as shown in Figure 12. As a result of the hydraulic interaction between John's Pass and Blind Pass, changes in the cross-sectional area of Blind Pass slightly affect the velocities at John's Pass (Fig. 12). The tidal prisms of the inlets and Boca Ciega Bay as a function of the cross-sectional area of Blind Pass are shown in Figures 13 and 14.

The cross-sectional area of John's Pass was measured to be 10,200 square feet. Maximum spring velocities in the main channel averaged 3.6 ft/sec and 3.4 ft/sec, averaged across the cross-section. Results of computer simulations in which the channel dimensions representing John's Pass channel were increased and then decreased are shown in Figure 15. Changes in the tidal prisms of each of the inlets and Boca Ciega Bay are shown in Figure 16 and 17.

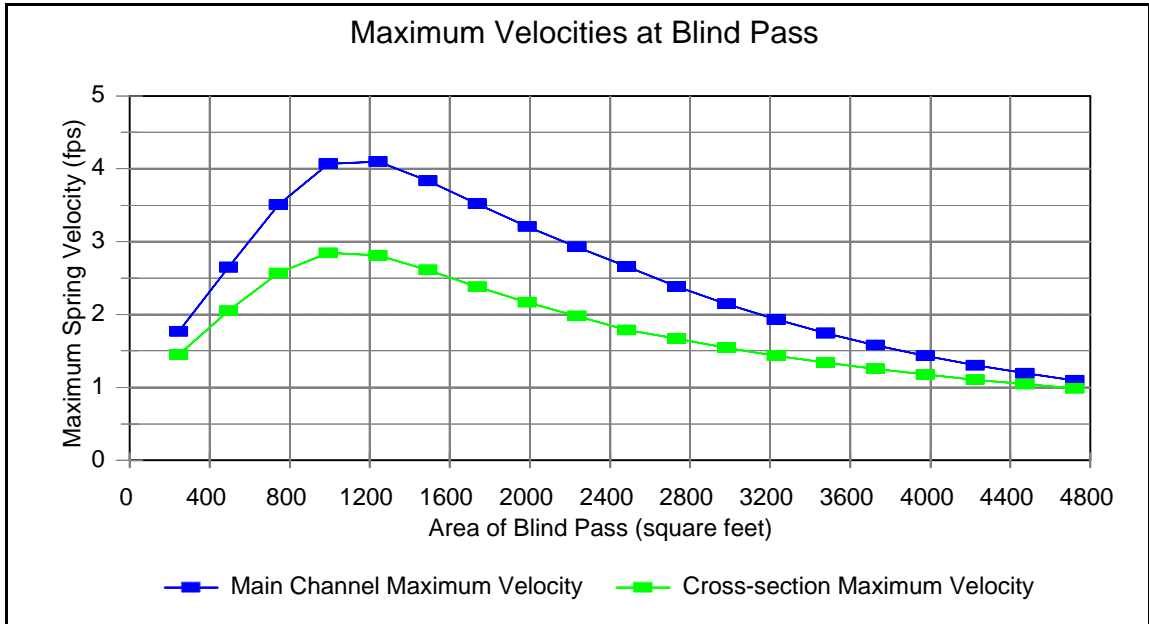
Stability diagrams of John's Pass and Blind Pass may be used to predict how each inlet responds to deposition and erosion of its channel. The stability diagram for Blind Pass indicates that the "critical area" for the inlet was approximately 1000 square feet. The associated spring velocity, averaged across the width of the inlet, was 2.8 feet per

second. For cross-sectional areas larger than the “critical area” but less than the equilibrium (measured) cross-sectional area, the inlet may be classified as scouring or “stable”(O’Brien and Dean, 1972). According to Escoffier’s (1940) original stability concept, tidal currents would tend to flush the inlet of sediments as a result of an increase in velocity. Consequently, the channel cross-sectional area would be maintained. An “unstable” condition would occur if the cross-sectional area of Blind Pass were less than approximately 1000 square feet. Model results show a sharp drop in the tidal prism of Blind Pass associated with such a reduction in the area of the inlet (Figure 13). It should be noted, however, that when the cross-sectional area of Blind Pass is greater than approximately 2000 square feet, velocities fall below 2 ft/sec and the ability of the current to move sediment may diminish.

The “critical area” for John’s Pass was approximately 6100 square feet with an associated, weighted velocity of 4.2 ft/sec (Fig. 15). The decrease in velocity at the “critical area” is linked to a significant reduction in the tidal prism of John’s Pass (Fig. 16).

Stability diagrams are based on the concept that maximum velocities resulting from changes in the cross-sectional area of a channel may be used to determine erosional or depositional tendencies of an inlet. They do not account for littoral drift, which may impede flow through a channel, or for changes in the distribution of sediment which may occur as a result of variations in the flow regime of the bay and inlets. Because flow through John’s Pass accounts for 40% of the tidal prism of Boca Ciega Bay (Table 6), a hypothetical scenario in which the area falls below 6100 square feet would result in a sharp drop in the tidal prism of the entire bay (Figure 17).

(a)



(b)

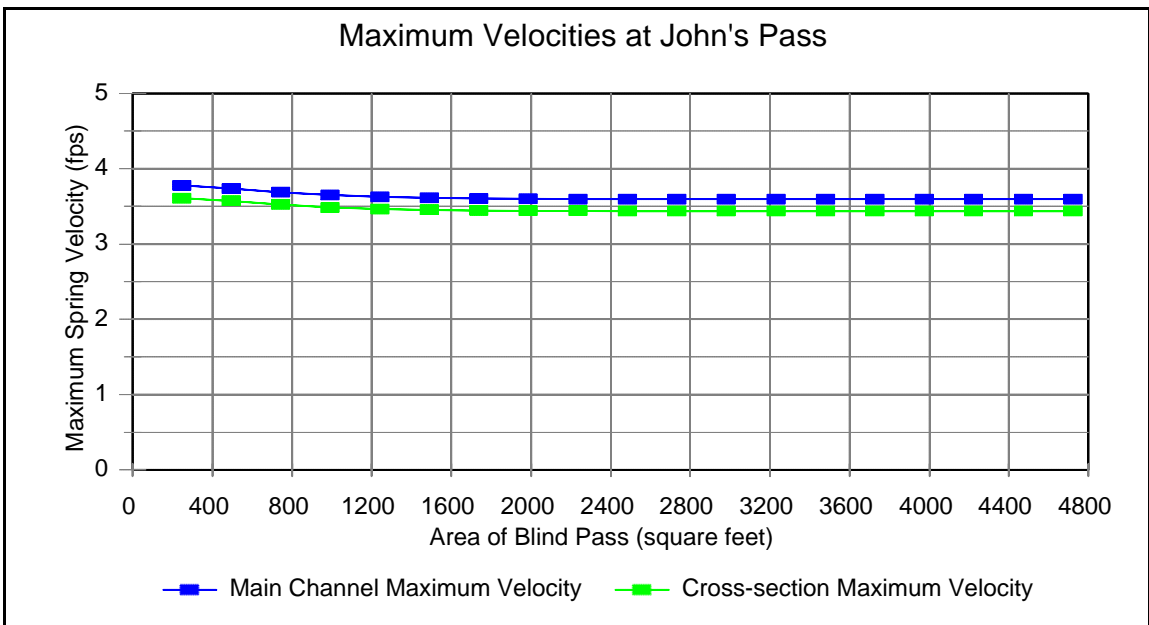
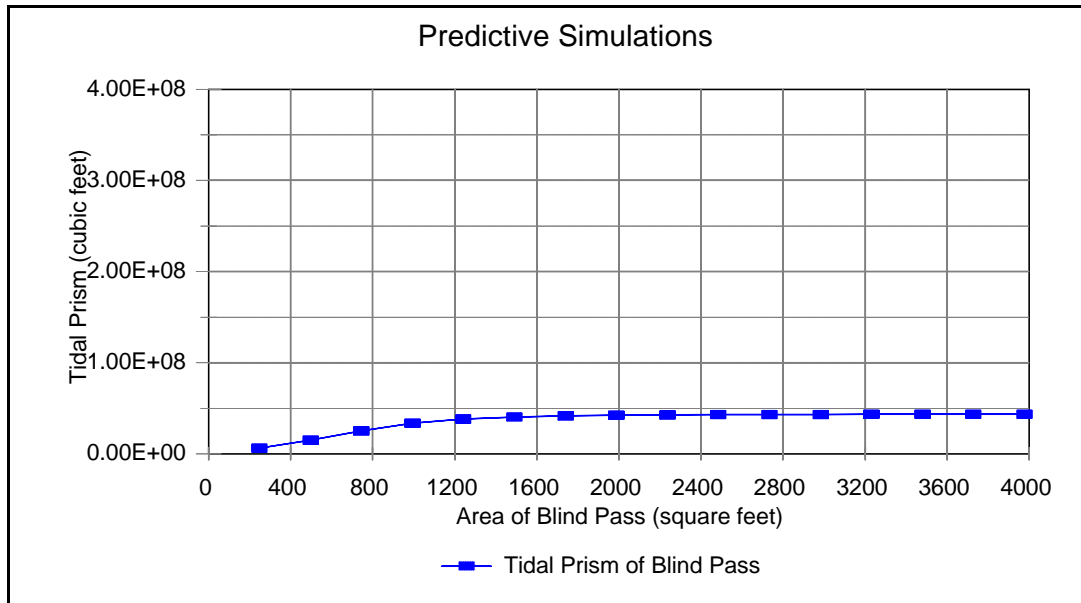


Figure 12. Stability diagram for (a) Blind Pass and (b) corresponding maximum velocities at John's Pass.

(a)



(b)

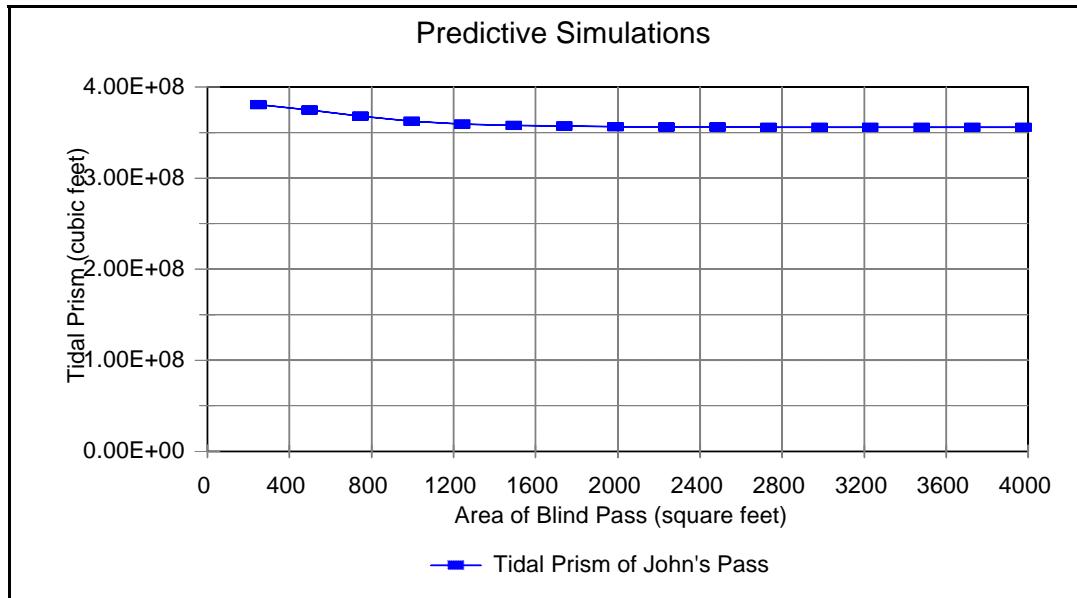


Figure 13. Tidal prisms of (a) Blind Pass and (b) John's Pass as a result of changes in the cross-sectional area of Blind Pass.

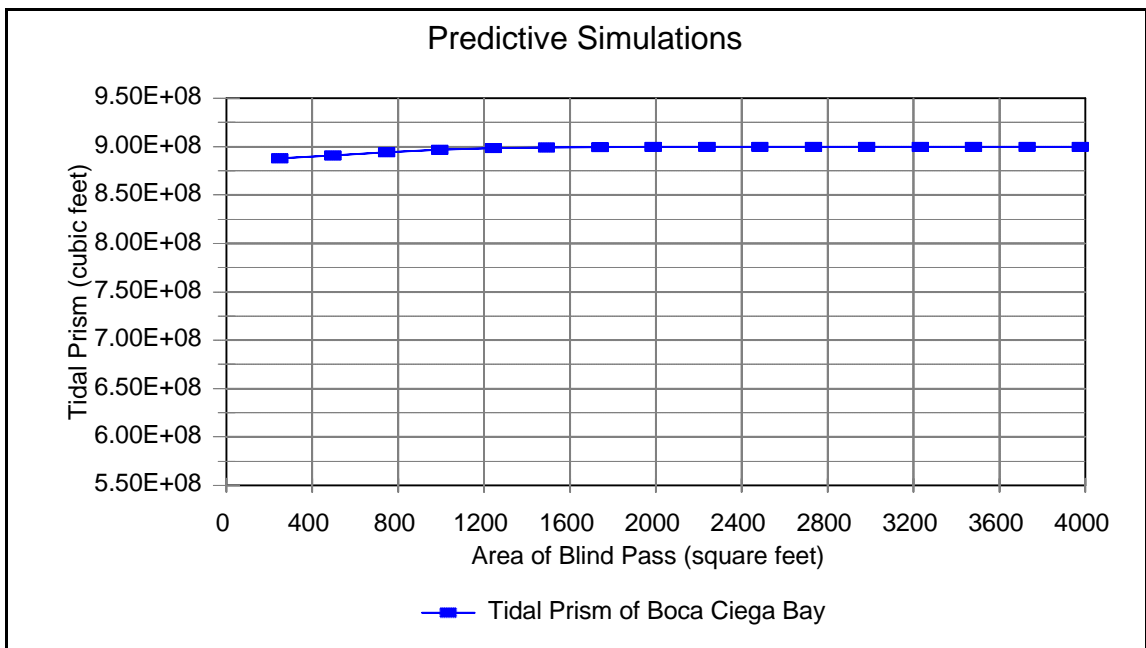
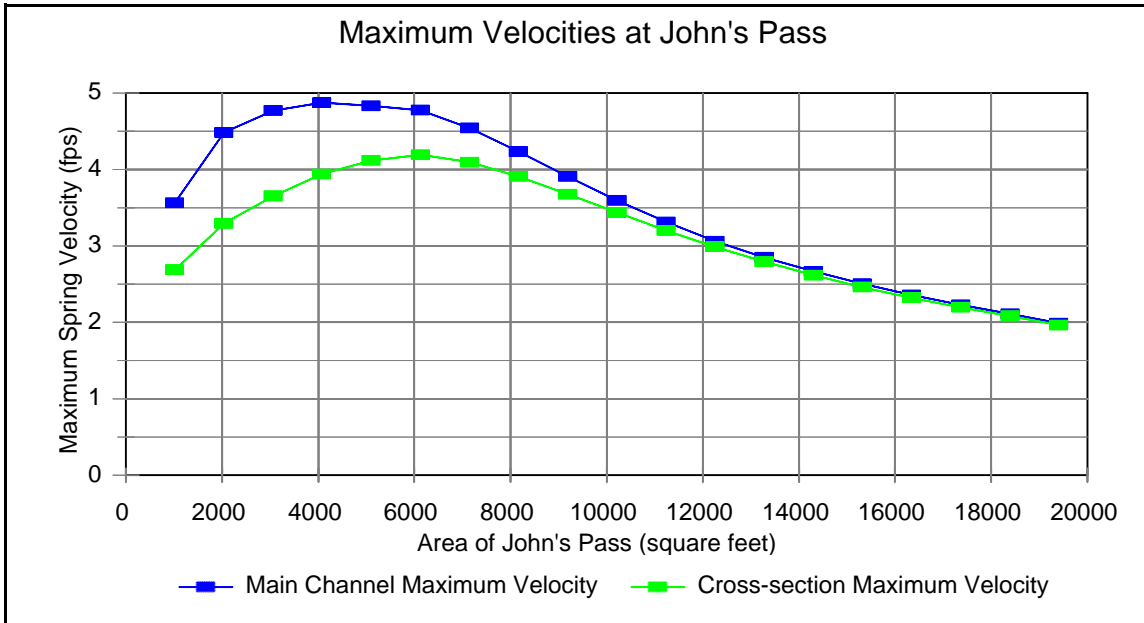


Figure 14. Tidal prism of Boca Ciega Bay as a result of changes in the cross-sectional area of Blind Pass.

(a)



(b)

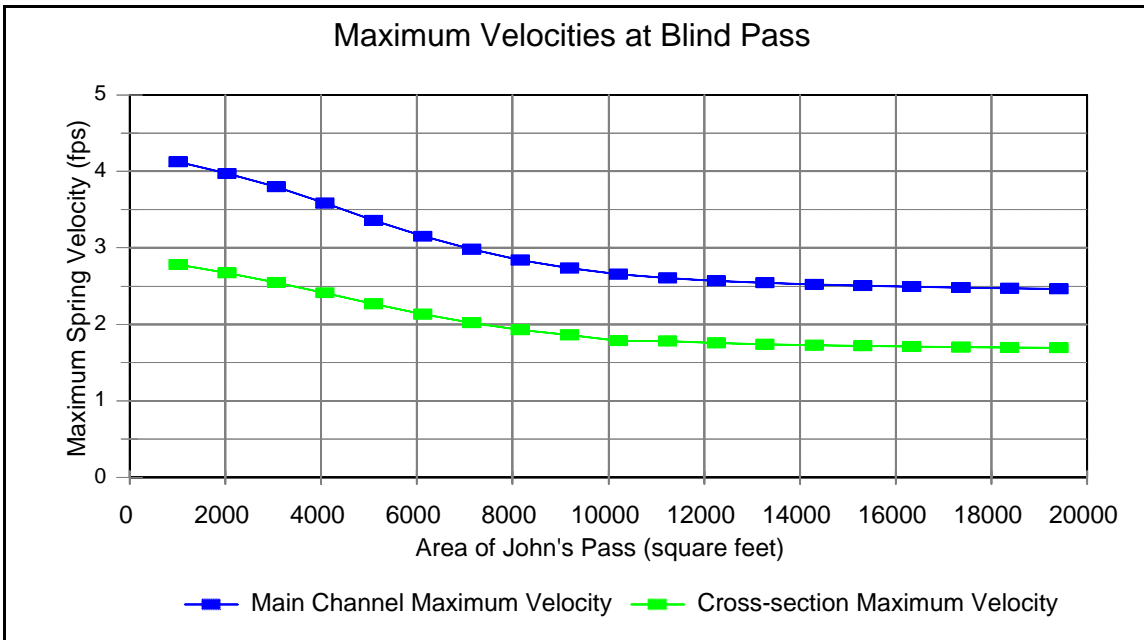
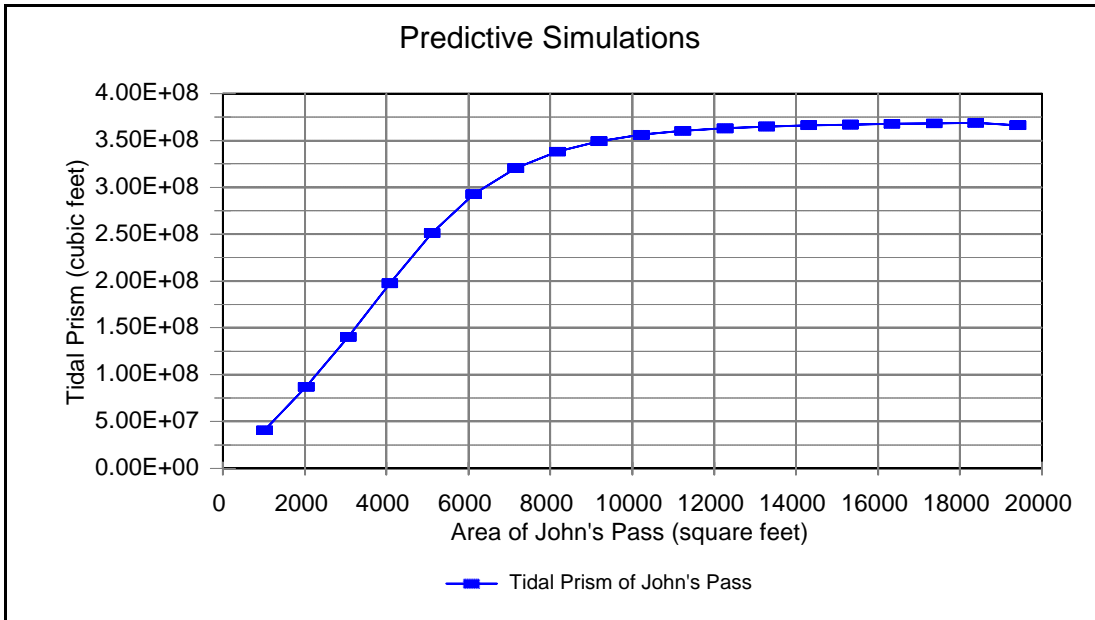


Figure 15. Stability diagram for (a) Johns' Pass and (b) corresponding maximum velocities at Blind Pass.

(a)



(b)

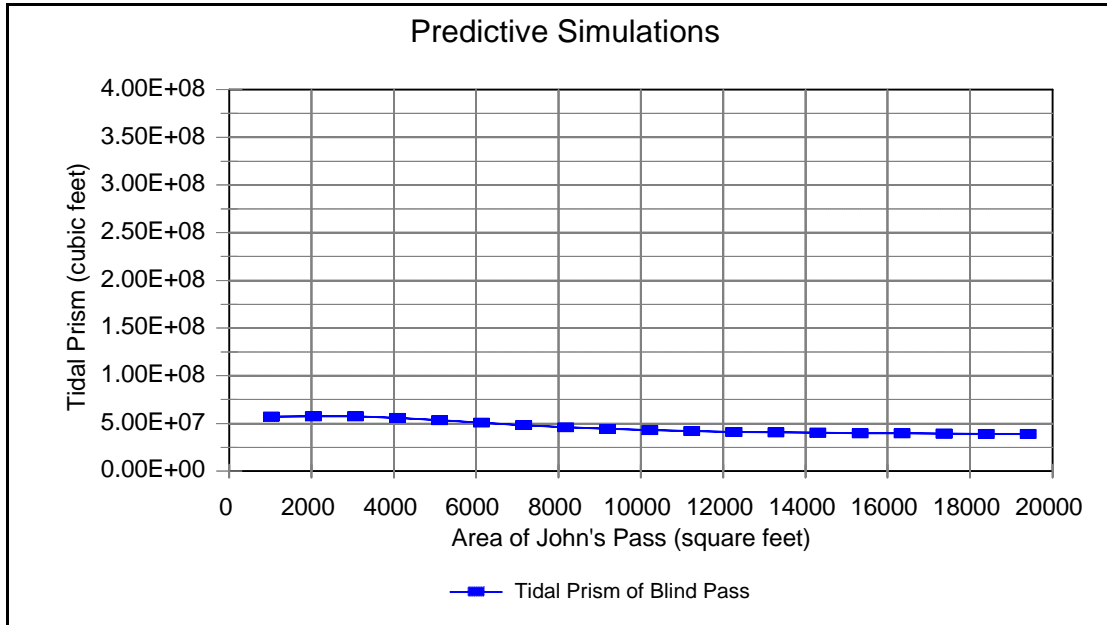


Figure 16. Tidal prisms of (a) John's Pass and (b) Blind Pass as a result of changes in the cross-sectional area of John's Pass.

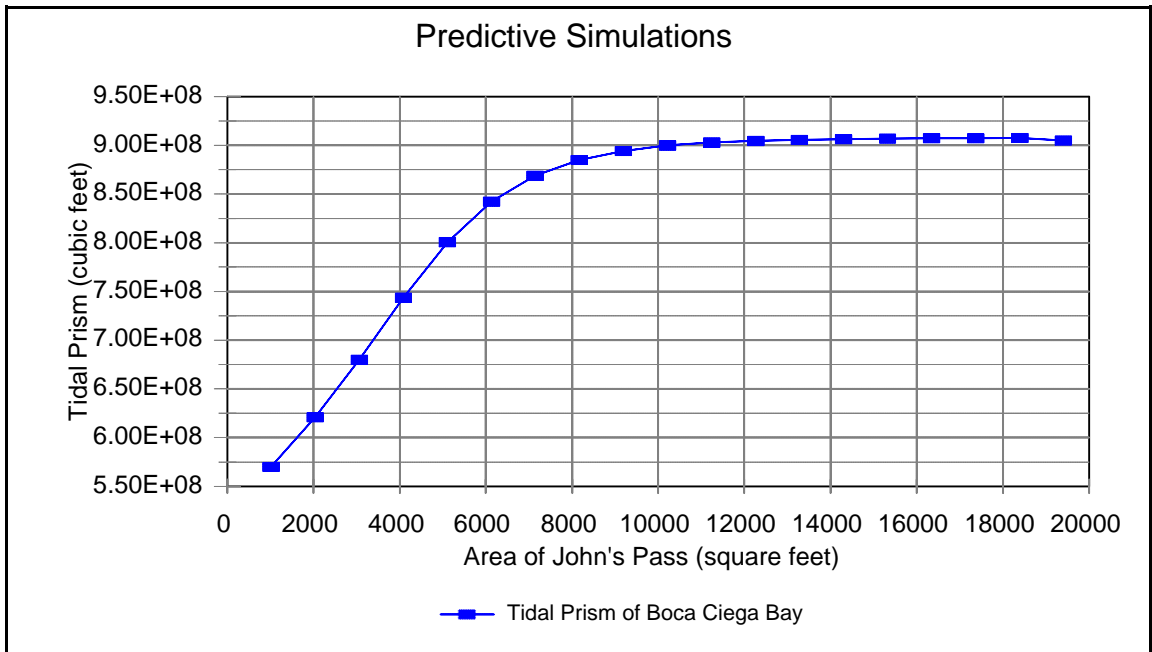


Figure 17. Tidal prism of Boca Ciega Bay as a result of changes in the cross-sectional area of John's Pass.

## Flow Regime of Boca Ciega Bay

Boca Ciega Bay is a tide-dominated embayment in which the hydraulic interaction between tidal inlets influences morphology. John's Pass, approximately four times the size of Blind Pass, carries more than eight times the tidal prism of Blind Pass and approximately forty percent of the tidal prism of Boca Ciega Bay. A history of the cross-sectional areas of the two inlets indicates that John's Pass has increased in size as the area of Blind Pass declined (Fig. 2). Analysis of results of the Boca Ciega Bay model shows that a co-dependency in the hydraulic characteristics of the two inlets also existed. The inverse relationship between the tidal prism of John's Pass and Blind Pass is depicted in Figures 13 and 16. Variations in maximum velocities and sediment-transport capacities at both passes are associated with these changes. Because only approximately 5% of the tidal prism of Boca Ciega Bay is fed through Blind Pass, changes in the area of the inlet do not substantially affect hydraulics at John's Pass. Variations in the area of John's Pass affect the tidal prism of the inlets as well as Boca Ciega Bay. As a result, changes in area of John's Pass have a greater affect on bay hydraulics. A change in the velocity at Blind Pass occurs as the area of John's Pass is reduced (Fig. 15).

## Stability of John's Pass

Current speeds generated by the Boca Ciega Bay model indicate that maximum spring velocities, weighted across the width of the inlet, reached an average of 3.4 ft/sec.,. A tidal-prism-to-littoral-drift ratio of 522 indicates that the inlet is hydraulically capable of flushing sediments from its channels (Table 3) so that its relatively high current speeds may be maintained. Stability diagrams which depict maximum velocities as a function of

the inlet's cross-sectional area also indicate that John's Pass is capable of scouring its channel (Fig. 15).

#### Stability of Blind Pass

At Blind Pass, peak velocities, weighted across the width of the channel, averaged 1.8 ft/sec. Although stability diagrams for Blind Pass (Fig. 12) indicate that current speeds would increase in response to inlet shoaling, relatively large quantities of littoral-drift material can prevent adequate scour of the pass. A tidal-prism-to-littoral-drift ratio of 34 (Table 3) suggests that relatively high volume of sand flux impedes flow within the inlet's channel. As a result of increased shoaling at the inlet, a gradually lengthening of the inlet's channel occurred. Because of the increase in channel length, current velocities as well as transport capabilities declined. Consequently, the cross-sectional area of Blind Pass gradually decreased with time. At Blind Pass, model results indicate that a gradual decrease in tidal prism occurs as the inlet's area has reduced (Fig. 13). As a result of a decline in the transport capacity of Blind Pass, the inlet is unable to naturally maintain its channel and periodic dredging is required.

## HYDRAULIC EVOLUTION OF BOCA CIEGA BAY

The morphology of Blind Pass indicates that the inlet was transformed from a mixed-energy pass to one dominated by deposition from wave-induced longshore transport. At the same time, a history of the cross-sectional area of John's Pass shows the pass has increased in size throughout most of its history. This increase is believed to have been caused by a decrease in the tidal prism of Blind Pass as well as the closure of Indian Pass in the 1920's (Mehta et al., 1976).

A simulation of the Boca Ciega Bay model in which the configuration of the bay and the cross-sectional areas of inlets broadly correspond to 1926 dimensions was run in order to characterize the hydraulic environment during the period. The cross-sectional area of John's Pass in 1926 was reportedly 5780 square feet; the area of Blind Pass was 2280 square feet (CPE, 1992). The entrance of Blind Pass was approximately 4000 feet north of its present location. Indian Pass was closed by this time. Dredge-and-fill islands had not yet been developed (Mehta et al., 1976). Although survey data from the early 1900's is limited and its accuracy is difficult to assess, a nautical chart of the region shows the general configuration of the bay before dredge-and-fill activities (USC&GS, 1885).

According to the model simulation of flow conditions in 1926 assuming offshore tidal conditions of today, maximum spring velocities were 6.8 ft/sec at John's Pass. The

spring tidal-prism at the inlet reached  $7.9E+8$  cubic feet, approximately 13% greater than in 1998. Relatively high velocities and the sizeable tidal prism carried by John's Pass suggest the inlet had a greater potential to scour in 1926 than after the development of dredge-and-fill islands. A computer simulation of a scenario in which the islands occupied the bay while the cross-sectional areas of Blind Pass and John's Pass corresponded to 1926 dimensions shows the result of development of the islands was a drop in the velocities to 5.9 ft/sec at John's Pass and a concurrent decrease in tidal prism. The model shows a decrease in scour potential at John's Pass as a result of the development of dredge-and-fill islands.

At Blind Pass, maximum spring velocities generated by the model representing 1926 conditions were 3.1 ft/sec. The tidal prism was  $1.5E+8$ , approximately 90% greater than the 1998 tidal-prism volume. According to the model, Blind Pass had a significantly greater ability to scour in the early 1900's than in its recent history.

The computer simulation of the scenario in which the islands occupied the bay while the cross-sectional areas corresponded to 1926 dimensions indicates that maximum velocities at Blind Pass dropped to approximately 1.9 ft/sec. According to the model, the placement of dredge-and-fill islands reduced the tidal prism of Blind Pass. Lower current velocities prevented adequate scour of the channel.

Because survey information of the study area in the early 1900's is very limited, current speeds produced by the historical computer simulations should be interpreted as estimates used to determine general trends associated with changes in the bay's configuration. Results show the development of dredge-and-fill islands decreased the tidal prism of Blind Pass and, as a result, its ability to flush its channels. Although a

portion of this prism would have been captured by John's Pass, an overall decrease in the tidal prism of John's Pass suggests the ability of the inlet to scour the channel lessened.

## CONCLUSIONS

The conclusions reached from results of a two-dimensional hydraulic model of Boca Ciega Bay, John's Pass, and Blind Pass were:

1. Peak spring velocities at John's Pass during the period of simulation were approximately 3.6 ft/sec in the main channel and 3.4 ft/sec, averaged across the width of the inlet. At the throat of Blind Pass, maximum spring velocities averaged 2.7 ft/sec in the main channel and 1.8 ft/sec, averaged across the inlet channel.

2. The average tidal prism of the bay during the time of simulation was approximately  $9E+8$  cubic feet. John's Pass carried approximately 40% of this volume; Pass-A-Grille inlet's northern channel (Vina del Mar E. and Vina del Mar W.) approximately 33% ; and Blind Pass approximately 5%. The remainder of the bay's tidal prism was distributed between channels at the Narrows Intracoastal Waterway and waterways north of Pass-A-Grille inlet (Fig. 4).

3. Net flow trends over the 11-day simulation showed inflow at John's Pass, Blind Pass, and Vina del Mar W. channels (Fig. 5). Net outflow occurred at the Narrows (Intracoastal Waterway), Vina del Mar E., Isla del Sol, and Cat's Point channels. The model indicated net flow over the study period was out of the bay; a drop in water levels at boundary channel locations was on the order of 0.1 ft.

4. Plots of the tidal prism versus the cross-sectional area of John's Pass and Blind Pass show that the relationship agrees closely with results of Jarrett's (1976) regression analysis.

5. The ratio of tidal prism to littoral drift at John's Pass was 522. According to Bruun's (1978) stability index, the inlet is capable of adequately flushing its channels; the stability of John's Pass may be rated as "good." The ratio of tidal prism to littoral drift at Blind Pass was 34. The inlet's stability was characterized as "poor."

6. Stability diagrams for John's Pass indicate the maximum velocity would increase if the cross-sectional area is reduced until the inlet reaches an area of approximately 6100 square feet. At this point, the tidal prism of John's Pass and Boca Ciega Bay would drop markedly. Further reductions in the inlet's area would result in lower current velocities. Stability diagrams for Blind Pass show the "critical area" is approximately 1000 square feet. If the inlet's size fell below this value, model results show velocities would decline, and the tidal prism of Blind Pass would drop sharply. The tidal prism of Boca Ciega Bay would not be significantly affected.

7. The tidal prisms of John's Pass and Blind Pass are inversely related. Because a relatively small percentage of the bay tidal prism is fed through Blind Pass, the influence of Blind Pass on scour tendencies at John's Pass is very minor. Changes in the size of John's Pass have a greater influence on hydraulic characteristics of the bay.

8. Based on limited survey data of the study area in the early 1900's, the model indicates the development of dredge-and-fill islands decreased the tidal prism of Blind Pass and, as a result, its ability to flush its channels. Although a portion of this prism would have been captured by John's Pass, an overall decrease in the tidal prism of John's Pass suggests its ability to scour its channel lessened.

9. Peak velocities resulting from a 100-year storm-surge simulation with barrier island overtopping were 7.2 ft/sec. for John's Pass and 3.2 ft/sec. for Blind Pass.

## REFERENCES

- Bruun, P. , 1978, *Stability of Tidal Inlet: Theory and Engineering*, Department of Port and Ocean Engineering, Developments in Geotechnical Engineering v. 23, Amsterdam, 510 p.
- Christensen, B.A., and Langley, T. B., “A fluvio-hydrographic survey of proposed marina site, John’s Pass,” Pinellas County, Florida, 1975.
- Coastal Planning & Engineering, Inc., (CPE), 1992, *Blind Pass Inlet Management Plan*, Pinellas County, Florida, 68 p.
- Coastal Technology Corporation (CTC), 1993, *John’s Pass Inlet Management Plan*, Pinellas County, Florida, 31 p.
- Davis, R.A., Jr., and Gibeaut, J.C., 1990, *Historical Morphodynamics of Inlets in Florida: Models for Coastal Zone Planning*, Florida Sea Grant College, Technical Paper 55, p.29-35.
- Dean, R. G., Chiu T. Y., Wang, S. Y., 1995, *Pinellas County Storm Surge Model Study*, “Combined Total Storm Tide Frequency Analysis for Pinellas County, Florida,” Florida Department of Environmental Protection, 63p.
- Escoffier, F. F., 1940. “The stability of tidal inlets,” *Shore and Beach*, Vol. 8, Number 4. p. 114-115.
- Escoffier, F. F., 1977. “Hydraulics and Stability of Tidal Inlets,” Department of Army Corps of Engineers, GITI Report 13, 76 p.
- Florida Design Consultants (FDC), 1997, “Pinellas County Map Hydrographic Survey,” 7 p.
- Jarrett, J. T., 1976, *Tidal Prism-Inlet Area Relationships*, Department of Army Corps of Engineers, GITI Report 3, 32 p.
- Loeb, W. A., 1994. “Beaches of Pinellas County, Florida: A History of their Comings and Goings (circa 1850-- present),” U.S. Department of the Interior U.S. Geological Survey. Center for Coastal Geology and Regional Marine Studies, p. 1.1-14.4.

- National Oceanic and Atmospheric Administration (NOAA), 1977. Nautical Chart.
- National Oceanic and Atmospheric Administration (NOAA), 1995. Nautical Chart.
- National Oceanic and Atmospheric Administration (NOAA), 1997. Nautical Chart.
- McKiernan, B.A., 1993, "Basic Hydraulics," in Zipparro, V. J., and Hasen, H.(eds.), *Davis' Handbook of Applied Hydraulics*, McGraw-Hill, Inc., New York, p. 2.1-2.33.
- Mehta, A. J., Adams, W. D., and Jones, C.P., 1976, *John's Pass and Blind Pass: Glossary of Inlets Report Number 4*, Florida Sea Grant Program, Report Number 18, 66 p.
- O'Brien, M., 1976, *Notes on Tidal Inlets on Sandy Shores*, Department of Army Corps of Engineers, GITI Report 7, 26 p.
- O'Brien, M. P., Dean, R. J., 1972, "Hydraulic and Sedimentary Stability of Coastal Inlets, Proceedings of the 13<sup>th</sup> Coastal Engineering Conference," ASCE, p. 761-780.
- Pitman-Hartenstein and Associates, Inc. (PH&A), 1997, *Scour Evaluation Report: John's Pass Boca Ciega Bay*, Tampa, Florida, 38 p.
- Ross, B., Ross, M., and Tara P., 1999, "USF-CMHAS Hydraulic and Water Quality Model (HYDQUAL) Documentation," University of South Florida, Tampa, FL, p. 1.1-1.68.
- United States Army Corps of Engineers (COE), 1997, *Project Condition Survey of Gulf Intracoastal Waterway Pinellas County*, Florida, 22 p.
- United States Army Corps of Engineers (COE), 1998, *Project Condition Survey of John's Pass Pinellas County*, Florida, 7 p.
- United States Coast and Geodetic Survey (USC&GS), 1885. Nautical Chart.
- Vincent, M., 1992, *John's Pass Scour Assessment Model*, The Center for Modeling Hydrologic and Aquatic Systems, University of South Florida, 57 p.

## APPENDICES

Appendix A. Section of Input Data Set

Boca Ciega Bay Spring Calibration

DT	LDRY	LCONV	LCOR	LUIIN	LBAR	LTIDE
9	1	0	1	0	0	1
TDAVG	TMANN	TFRIC				
0	0	0				
THPRNT	TUVD	TTROUT				
100	0	0				
NGATES	NDELH	NHGPTS	NTRPTS			
192	0	0	0			

GATES

Gate Number	Cell I	Cell J	Channel Side	Chan1 Depth	Chan1 Width	Chan2 Depth	Chan2 Width	Barrier Height	k
Narrows									
North of Bridge 1 (Narrows)									
1	34	1	1	-5	300	0	0	6	0
2	35	1	1	-5	300	0	0	6	0
3	36	1	1	-5	300	0	0	6	0
4	37	1	1	-5	300	0	0	6	0
Bridge 1									
5	38	1	1	-6	200	0	0	6	0.5
Channel South of Bridge 1 (Narrows)									
6	39	1	1	-5	300	0	0	6	0
7	40	1	1	-5	400	0	0	6	0
8	41	1	1	-5	350	0	0	6	0
9	42	1	1	-5	200	0	0	6	0
10	38	2	2	0	0	0	0	6	0
11	39	2	2	0	0	0	0	6	0
12	40	2	2	0	0	0	0	6	0
13	41	2	2	0	0	0	0	6	0
14	42	2	2	-4	300	0	0	6	0
15	42	3	2	-3	400	0	0	6	0
16	42	3	1	-5	350	0	0	6	0
17	40	5	1	-7	300	0	0	6	0
18	40	5	2	-7	300	0	0	6	0
19	41	4	1	-7	300	0	0	6	0
20	41	4	2	-7	300	0	0	6	0
Conch Key									
21	41	3	1	0	0	0	0	6	0
22	40	4	2	0	0	0	0	6	0
23	40	4	1	0	0	0	0	6	0
24	40	6	2	0	0	0	0	6	0
25	41	5	1	0	0	0	0	6	0
26	41	5	2	0	0	0	0	6	0

Appendix A. (Continued)

North Redington Beach

27	37	11	2	0	0	0	0	6	0
28	38	11	1	0	0	0	0	6	0
29	37	13	2	0	0	0	0	6	0

Lake Seminole

30	16	14	2	-2	0	0	0	6	0.5
----	----	----	---	----	---	---	---	---	-----

West of Bridge 3

31	33	28	1	0	0	0	0	6	0
----	----	----	---	---	---	---	---	---	---

Bridge 3 (Welch Causeway)

32	31	28	2	-10	100	0	0	-8	0.5
33	32	28	2	-8	14	0	0	6	0.5

Little Basin East of Bridge 3

34	26	28	1	-4	50	0	0	6	0
35	26	28	2	0	0	0	0	6	0
36	25	29	2	0	0	0	0	6	0

Long Bayou South

Bridge 4

37	16	32	1	-9	427	0	0	-2	0.5
38	16	33	1	-2	385	0	0	6	0.5
39	15	34	2	0	0	0	0	6	0

Crystal Island Northeast of Bridge 3C

40	27	33	2	-7	300	0	0	6	0
41	27	34	2	0	0	0	0	6	0
42	28	34	1	0	0	0	0	6	0
43	27	35	1	0	0	0	0	6	0
44	27	36	2	0	0	0	0	6	0

Bridge 3C

45	30	37	2	-8	47	0	0	6	0.5
----	----	----	---	----	----	---	---	---	-----

Crystal Island Southeast of Bridge 3C

46	30	38	2	0	0	0	0	6	0
47	29	38	1	0	0	0	0	6	0
48	29	39	2	0	0	0	0	6	0

John's Pass Flood Shoal

49	29	40	1	-6	300	0	0	-1	0
50	28	40	1	-5	200	0	0	-1	0
51	27	40	1	-4	350	0	0	-1	0
52	26	40	1	-5	400	0	0	-1	0
53	24	40	1	-6	400	0	0	-1	0
54	29	41	2	-14	175	0	0	-11	0
55	29	42	2	-11	200	0	0	-7	0
56	30	42	2	-12	200	0	0	6	0
57	26	42	2	0	0	0	0	6	0
58	29	41	1	-4	300	0	0	-1	0

Appendix A. (Continued)

59	28	41	1	-5	300	0	0	-1	0
60	27	41	1	-7	300	0	0	-1	0
61	26	41	1	-6	450	0	0	-1	0
62	28	40	2	0	0	0	0	3	0
63	27	40	2	0	0	0	0	3	0

Turtle Crawl Pt.

64	18	39	2	0	0	0	0	3	0
65	19	39	1	-2	100	0	0	3	0
66	17	39	2	0	0	0	0	3	0
67	16	39	2	0	0	0	0	3	0
68	21	40	1	0	0	0	0	4	0
69	18	41	1	-2	100	0	0	3	0

John's Pass

Bridge 5

70	33	43	1	-40	120	-14	387	93	0.5
71	33	44	2	-17	300	-9	299	0	0
72	32	43	1	-22	300	0	0	-16	0
73	31	44	2	-18	350	0	0	6	0
74	34	44	1	-13	600	0	0	0	0
75	34	43	1	-4	600	0	0	0	0

Channel between John's Pass Flood Shoal and Capri Isle

76	25	45	1	-12	200	0	0	-2	0
77	26	45	1	-12	200	0	0	-2	0
78	27	45	1	-12	200	0	0	-2	0
79	28	45	1	-12	200	0	0	-2	0
80	29	45	1	-12	200	0	0	-2	0
81	29	45	2	-12	200	0	0	-2	0
82	30	44	1	-12	200	0	0	-2	0
83	31	44	1	-6	200	0	0	6	0

Channel from John's Pass to Bridge 6

84	31	45	2	-15	50	-3	150	6	0
85	31	46	2	-15	50	-3	150	6	0
86	31	47	2	-13	50	-4	150	6	0
87	31	48	2	-12	50	-4	350	6	0
88	31	49	2	-12	50	-3	110	6	0
89	31	49	1	-8	50	-5	110	6	0

Channel Southeast of Bridge 6

90	30	50	1	-6	50	-3	240	6	0
91	29	50	1	-6	50	-3	240	6	0
92	28	50	1	-6	50	-3	240	6	0
93	27	50	1	-6	50	-3	240	6	0
94	26	50	1	-6	50	-3	240	6	0

Appendix A. (Continued)

95	25	50	1	-6	50	-3	240	6	0
96	24	50	1	-6	50	-3	240	6	0
South Sunshine Beach									
Bridge 6									
97	30	50	2	-7	48	0	0	6	0.5
98	30	51	2	-6	160	0	0	8	0
Bridge 7									
99	30	52	2	-4	23	0	0	6	0.5
100	30	53	2	-6	220	0	0	6	0
101	30	53	1	-6	200	0	0	6	0
Channel Southeast of Bridge 7									
102	24	53	1	-8	50	-6	549	0	0
103	25	53	1	-8	50	-2	549	0	0
104	26	53	1	-8	50	-2	549	0	0
105	27	53	1	-8	50	-2	549	0	0
106	28	53	1	-8	50	-2	549	0	0
107	29	53	1	-8	50	-3	549	0	0
Treasure Island									
North of Bridge 8									
108	27	54	2	0	0	0	0	-0.5	0
109	27	54	1	-6	400	0	0	-0.5	0
110	25	54	2	0	0	0	0	-0.5	0
111	26	54	1	-5	300	0	0	-0.5	0
112	26	54	2	-5	400	0	0	-0.5	0
Bridge 8									
113	27	55	2	-8	362	0	0	5	0.9
Shoal North of Bridge 10									
114	18	57	2	0	0	0	0	1	0
South of Bridge 8									
115	28	57	2	-5	350	0	0	8	0
North of Bridge 9									
116	23	54	1	-4	350	0	0	6	0
117	23	55	1	-4	350	0	0	6	0
118	23	55	2	-3	350	0	0	6	0
Bridge 9									
119	22	58	2	-10	600	0	0	0	0.5
120	21	58	2	-5	300	0	0	8	0.5
Southeast of Bridge 9									
121	22	59	1	0	0	0	0	6	0
122	22	59	4	0	0	0	0	6	0
123	21	59	2	0	0	0	0	6	0
Bridge 10									
124	17	60	2	-7	209	0	0	5	0.5

Appendix A. (Continued)

South Causeway Isles

Marker 9 to Obstruction (T3)

125	27	67	1	-10	100	0	0	-2	0
126	26	67	1	-8	100	0	0	-2	0
127	25	67	1	-8	100	0	0	-2	0
128	24	67	2	-4	100	0	0	-3	0
129	24	66	1	-4	100	0	0	-3	0
130	23	66	1	-8	100	0	0	-3	0
131	22	66	1	-12	100	0	0	-3	0

Channel to Bridge 10 (T4)

132	21	66	2	-12	100	0	0	-3	0
133	21	65	2	-4	100	0	0	-3	0
134	21	64	1	-4	300	0	0	6	0
135	20	64	1	-4	100	0	0	-4	0
136	19	64	1	-4	100	0	0	-4	0
137	18	64	2	-10	100	0	0	-4	0
138	18	63	2	-10	100	0	0	-4	0
139	18	62	2	-10	100	0	0	-4	0
140	18	61	1	-8	100	0	0	-4	0
141	17	61	2	-12	100	0	0	-3	0
142	24	65	1	0	0	0	0	6	0

Bridge 10A

143	22	64	2	-6	70	0	0	6	0.5
-----	----	----	---	----	----	---	---	---	-----

Blind Pass

North of Blind Pass

144	30	63	2	-4	300	0	0	6	0
145	30	62	2	-5	400	0	0	-2	0

Shoal E. of Blind Pass

146	29	62	1	-4	300	0	0	8	0
147	30	62	1	-3	300	-1	300	0	0

Bridge 11

148	30	64	2	-12	80	-3.5	450	8	0.9
149	31	71	2	-17	75	-8.5	185	8	0
150	31	72	2	-17	75	-8.5	185	8	0
151	31	73	2	-17	75	-8.5	185	8	0
152	31	74	2	-17	75	-7	173	8	0
153	32	74	1	-17	75	-7	455	8	0
154	33	74	1	-11	280	0	0	-3	0
155	32	75	2	-14	400	0	0	6	0
156	33	75	1	-8	400	0	0	-2	0
157	34	75	1	-8	400	0	0	-2	0

Appendix A. (Continued)

Corey Cswy.

Bridge 12

158	25	73	2	-11	93	-8	329	8	0.5
159	25	72	1	0	0	0	0	8	0

Gate near Bridge 12

160	25	73	1	-10	200	-8	399	0	0
-----	----	----	---	-----	-----	----	-----	---	---

North of Bridge 13

161	24	69	2	-9	480	0	0	8	0
162	24	70	2	-9	550	0	0	8	0
163	24	71	2	-9	480	0	0	8	0

Bridge 13

164	24	72	2	-10	27	-5	166	8	0.5
-----	----	----	---	-----	----	----	-----	---	-----

South of Bridge 13

165	23	72	1	-4	560	0	0	8	0
166	23	73	2	-4	450	0	0	8	0
167	24	73	2	-7	550	0	0	-2	0

Channel to Bridge 14

168	24	73	1	-8	50	-4	549	0	0
169	23	73	1	-8	50	-4	549	0	0
170	22	73	1	-8	50	-4	549	0	0

North of Bridge 14 ("NORTH BRIDGE")

171	22	70	2	-8	500	0	0	8	0.5
172	22	71	2	-5	300	0	0	8	0

Bridge 14

173	22	72	2	-10	100	-7	424	8	0.9
-----	----	----	---	-----	-----	----	-----	---	-----

Bridge 14A

174	21	74	2	-5	56	0	0	8	0.5
-----	----	----	---	----	----	---	---	---	-----

Vina Del Mar

Bridge 15A

175	27	89	2	-2	47	0	0	6	0.5
-----	----	----	---	----	----	---	---	---	-----

Bridge 15

176	26	98	2	-13	100	-11	499	0	0.5
177	25	98	2	-9	450	0	0	6	0.5
178	27	98	2	-6	300	0	0	6	0

Bridge 16

179	34	102	2	-8	276	0	0	6	0.5
-----	----	-----	---	----	-----	---	---	---	-----

South of Bridge 16

180	35	104	2	-2	600	0	0	0	0
-----	----	-----	---	----	-----	---	---	---	---

Isla del Sol

Bridge 17

181	16	99	2	-8	320	0	0	8	0.5
-----	----	----	---	----	-----	---	---	---	-----

Appendix A. (Continued)

Bridge 18

182            11    100   2                    -8    406    0            0            8    0.5

Boundary Conditions

183            24    105   4                    0     0     0            0            8    0  
 184            25    105   4                    0     0     0            0            8    0  
 185            30    105   4                    0     0     0            0            8    0  
 186            31    105   4                    0     0     0            0            8    0  
 187            32    105   4                    0     0     0            0            8    0  
 188            27     72   1                   -10   550   0            0            8    0  
 189            26     70   2                    0     0     0            0            8    0

Gate South of Bridge 17

190            16    100   2                    -9     50    -7           549           0    0

Hydraulic Loss Gates

191            27    42    3                    -6    600   0            0            0    0  
 192            37    45    1                   -12   600   0            0            0    0

Tide Section

hstart

1.03

nowsegs ntides

6    1

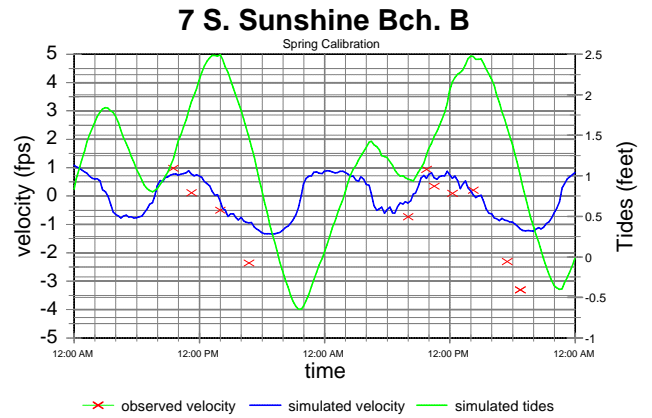
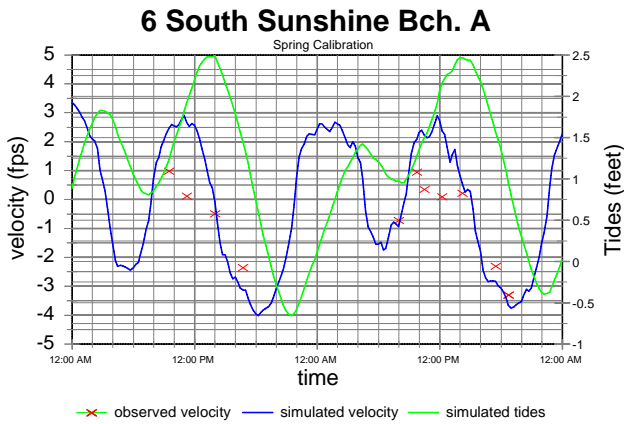
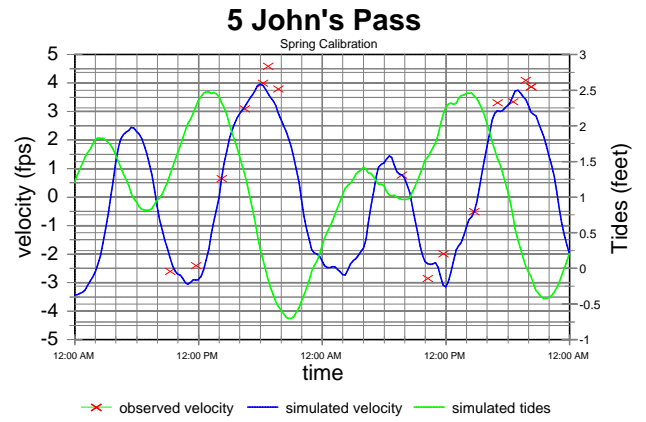
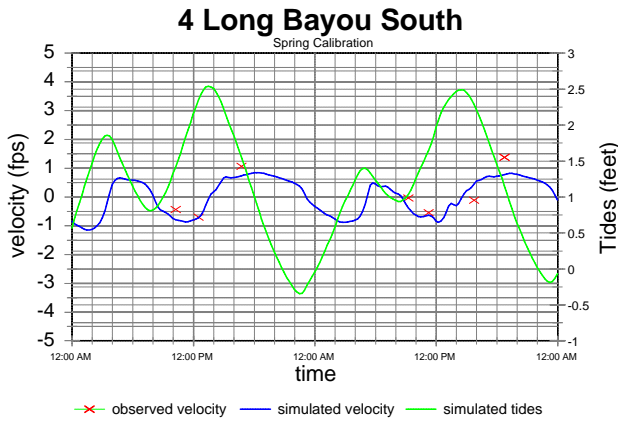
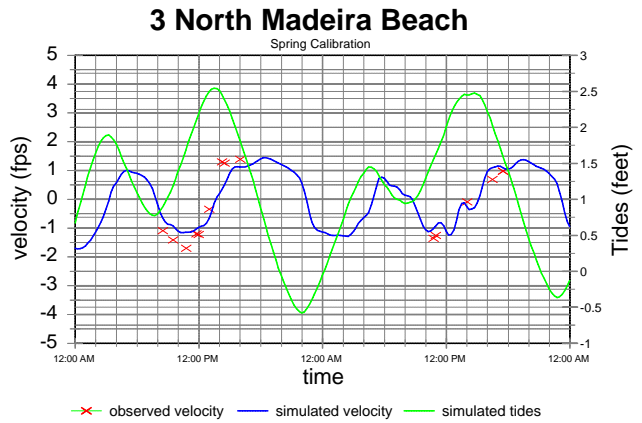
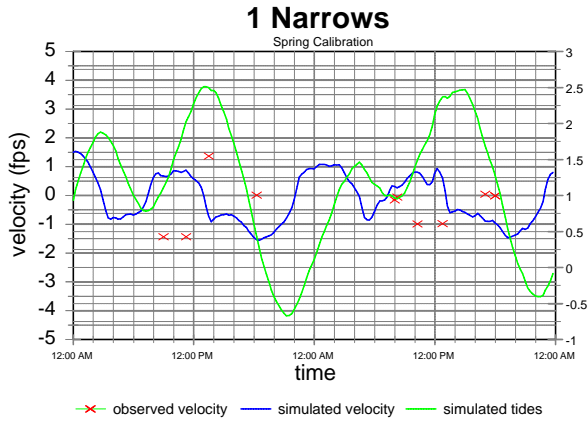
c south1 south2 south3 west1 west2 north

1    1    1    1    1    1    tide function to use  
 4    4    4    3    3    2    side to apply tide function  
 9    26   33   1    45   33    kstart, data lagged on Pass-A-Grille"  
 22   29   45   44   104   34    kstop  
 1    1    1    1    1    1    hamp

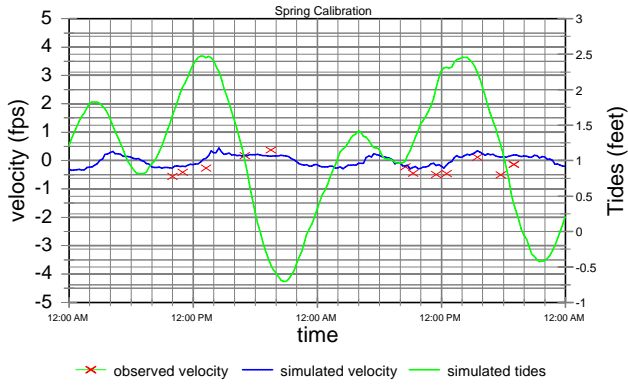
lags are negative leads are positive

-90   -41.69   -30.1   26    15   -25    dtstrt  
 -75   -32.15   0    16    2   -25    dtstop  
 0    0    0    0    0    0    dhrate  
 0.998   0.998   0.998   0.998   0.998   0.998    ampoff  
 0    0    0    0    0    0    refoff

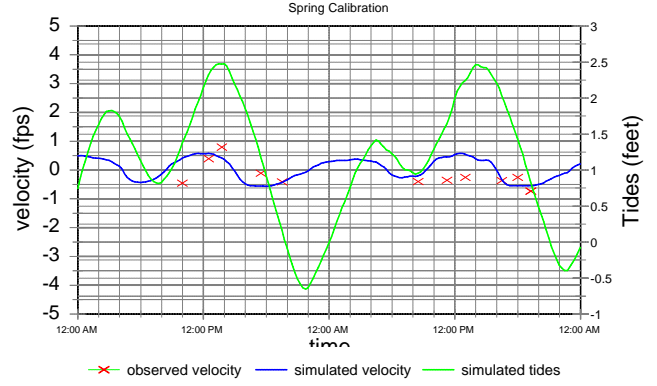
## Appendix B: Spring-tide Calibration



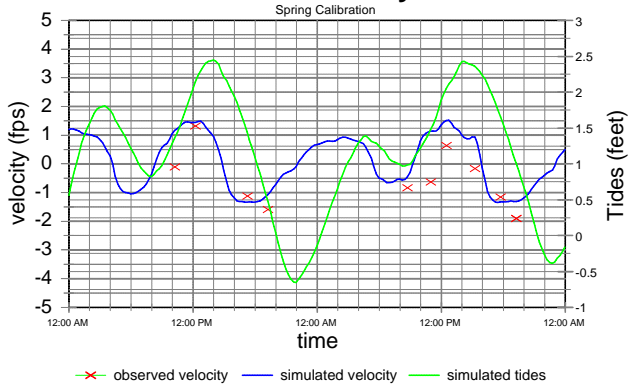
### 8 Treasure Island



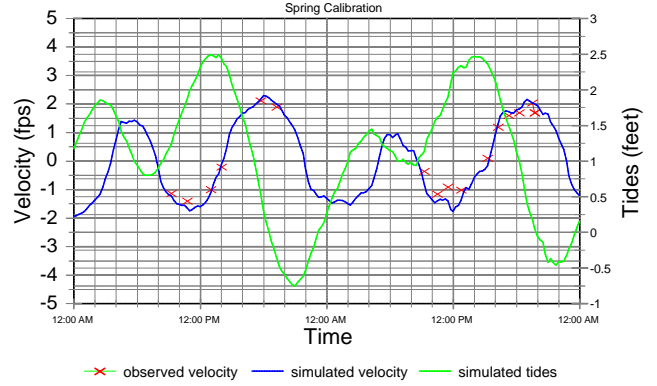
### 9 Paradise Island E.



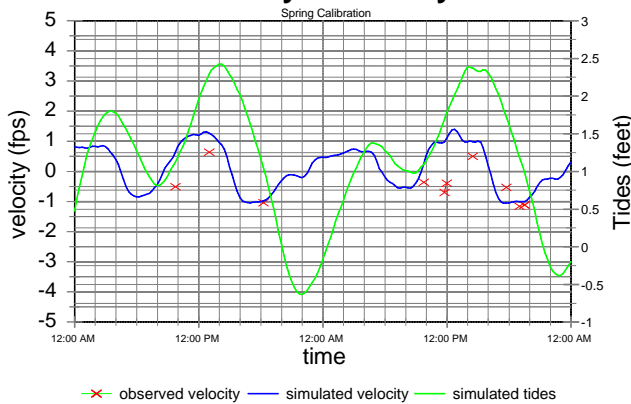
### 10 South Causeway Isl. E.



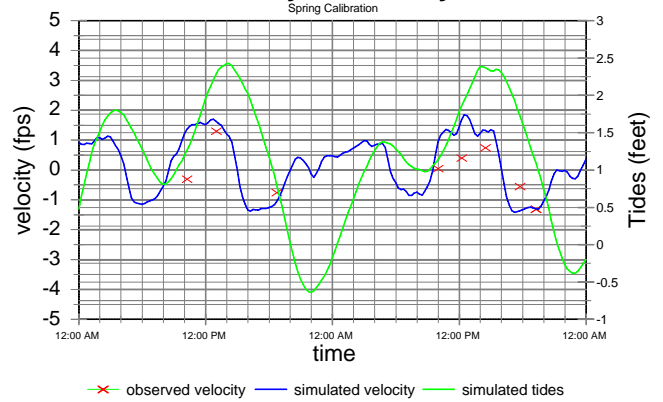
### 11 Blind Pass



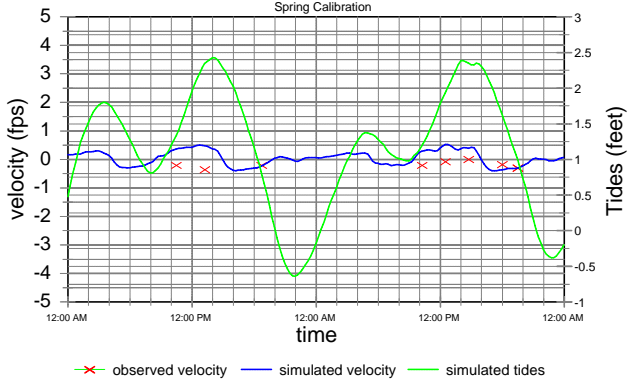
### 12 Corey Causeway A



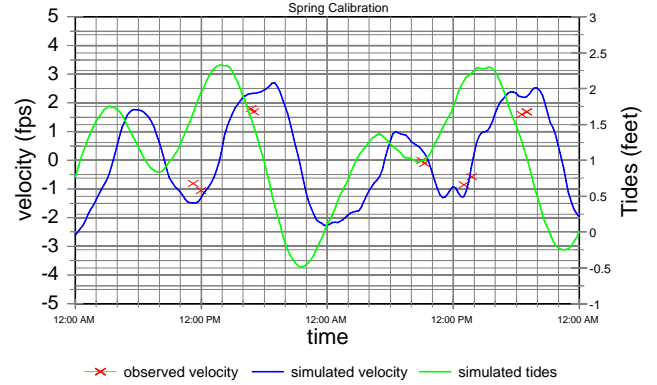
### 13 Corey Causeway B



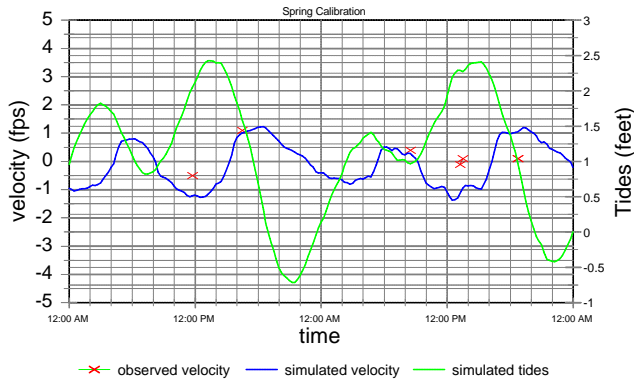
### 14 Corey Causeway C



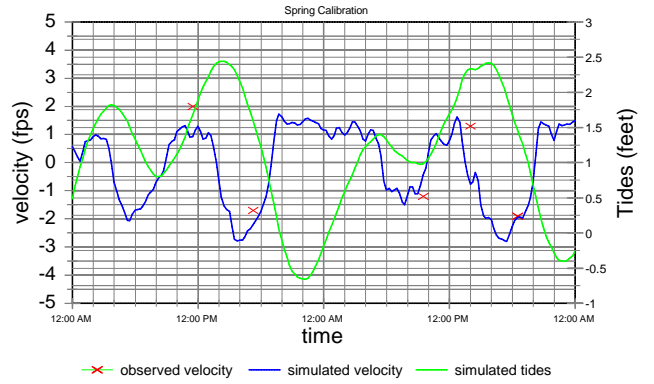
### 15 Vina del Mar E.



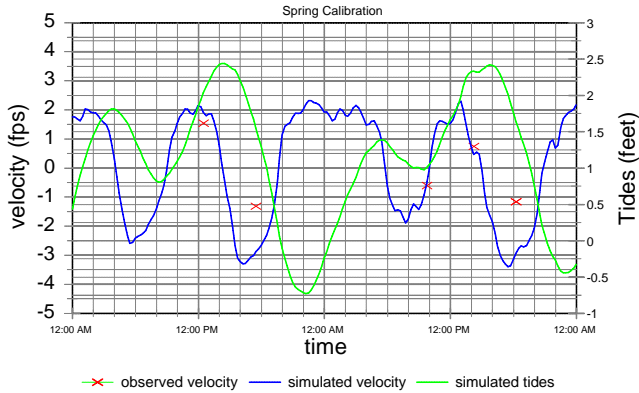
### 16 Vina del Mar W.



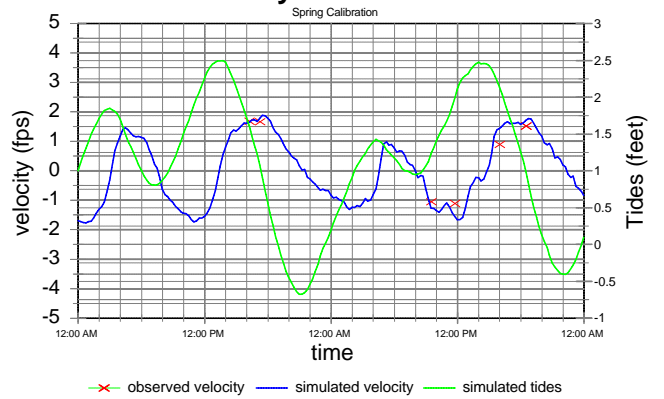
### 17 Isla del Sol



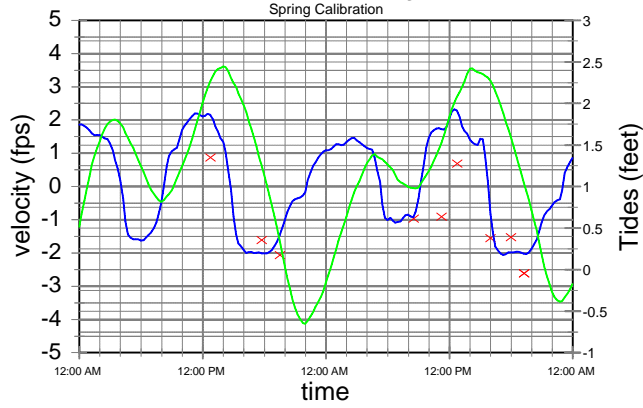
### 18 Cat's Point



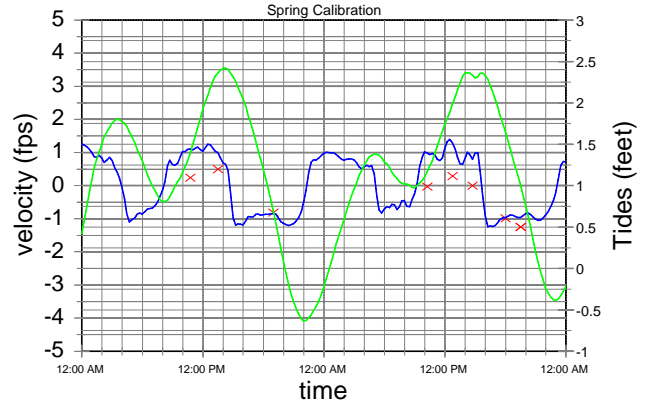
### 3C Crystal Island C



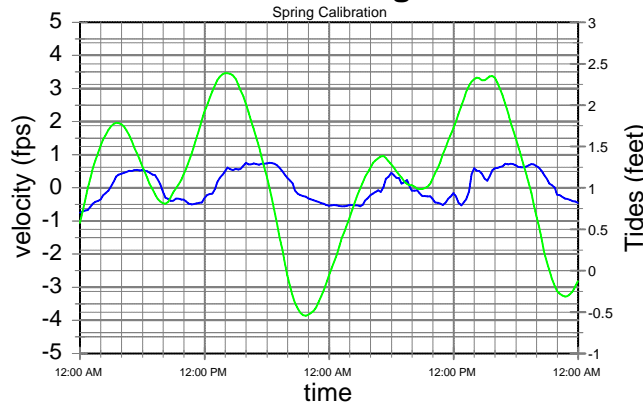
### 10A S. Causeway Isl. S.



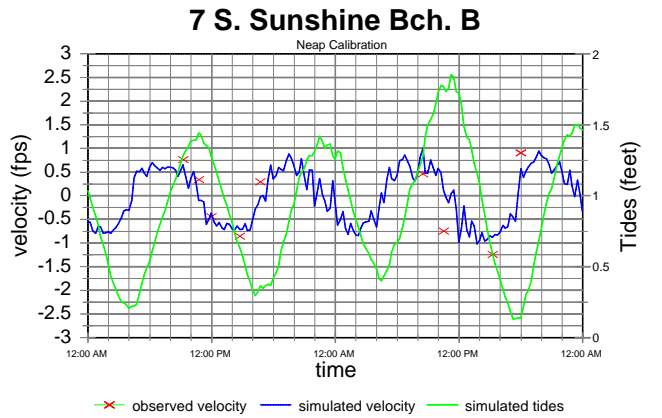
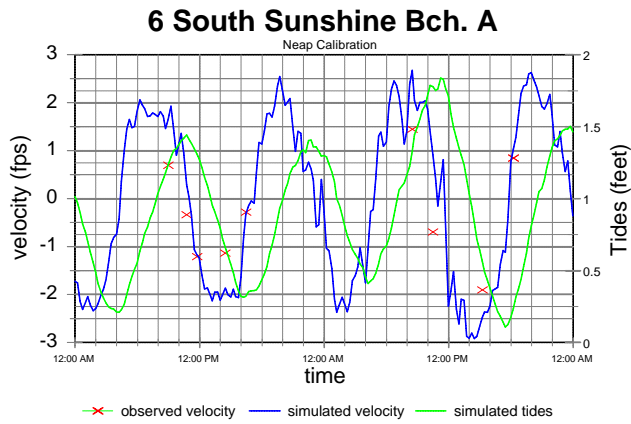
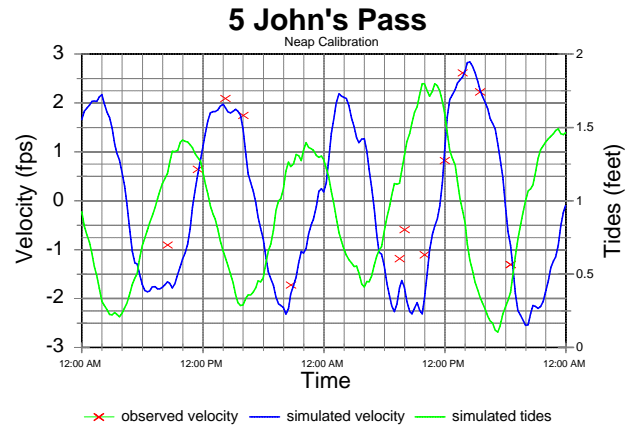
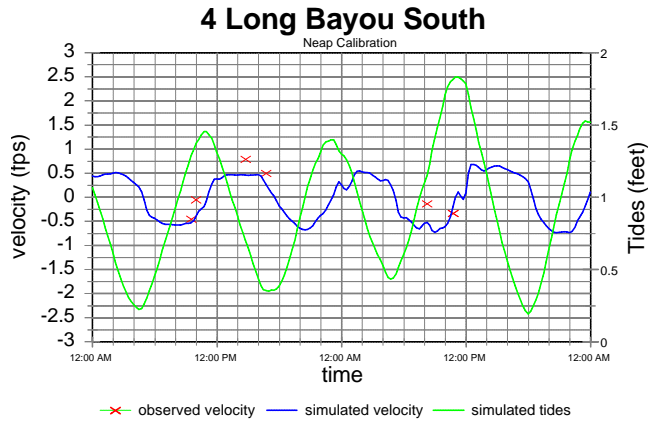
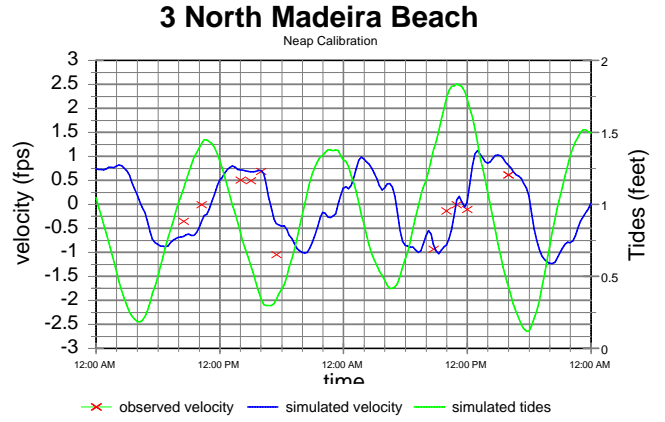
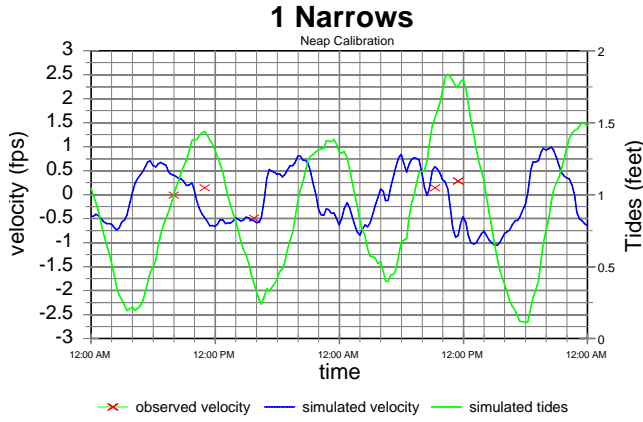
### 14A Paradise Isle



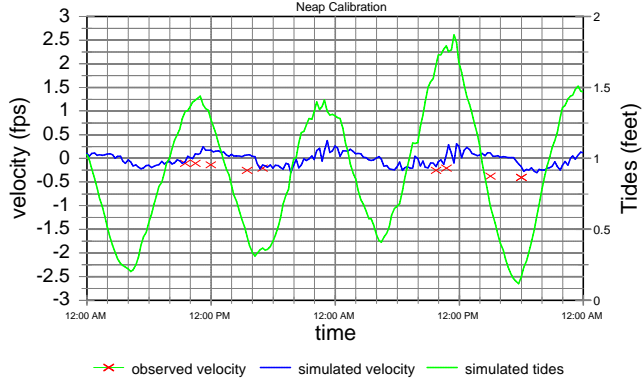
### 15A Boca Ciega Isle



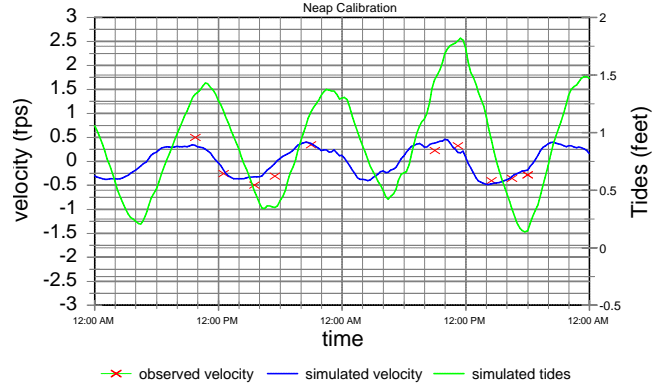
# Appendix C: Neap-tide Calibration



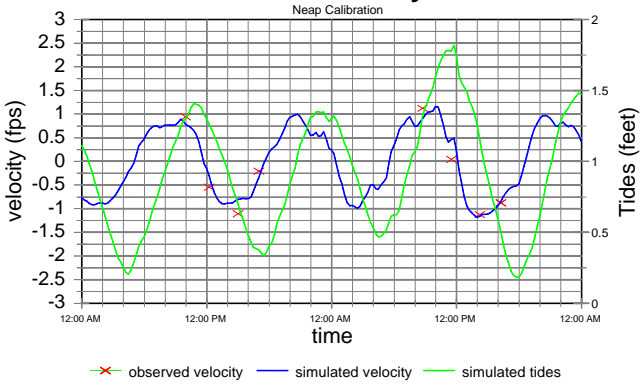
### 8 Treasure Island



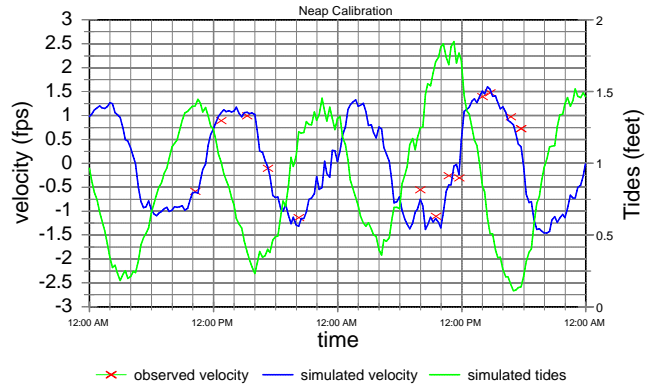
### 9 Paradise Island E.



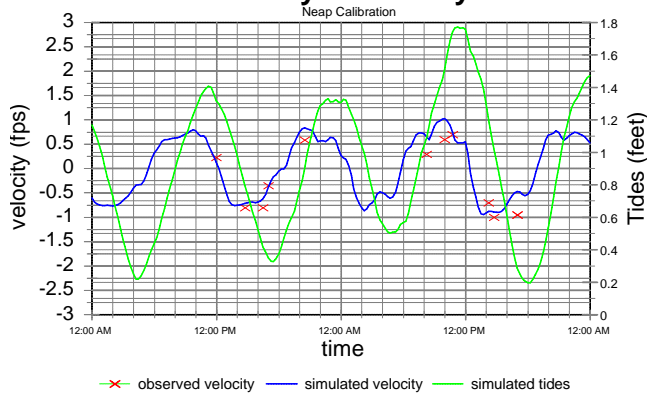
### 10 South Causeway Isl. E.



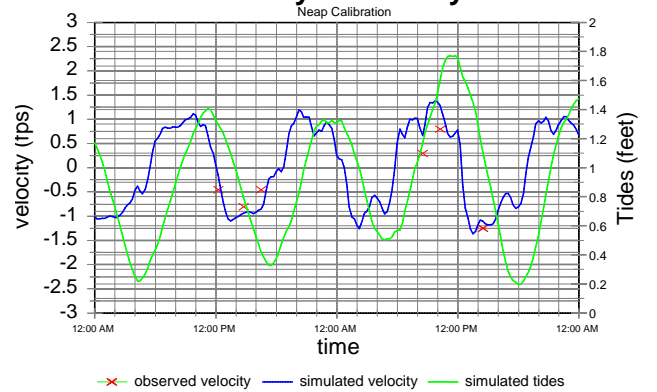
### 11 Blind Pass



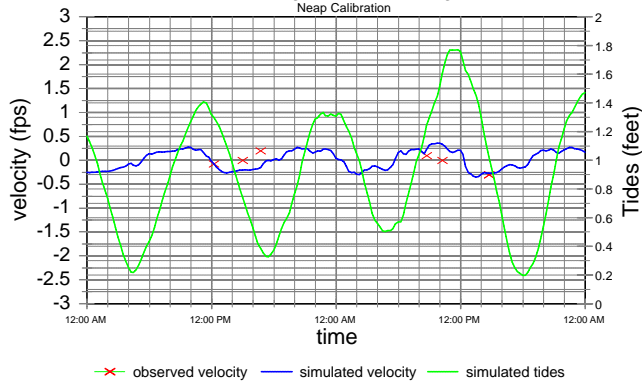
### 12 Corey Causeway A



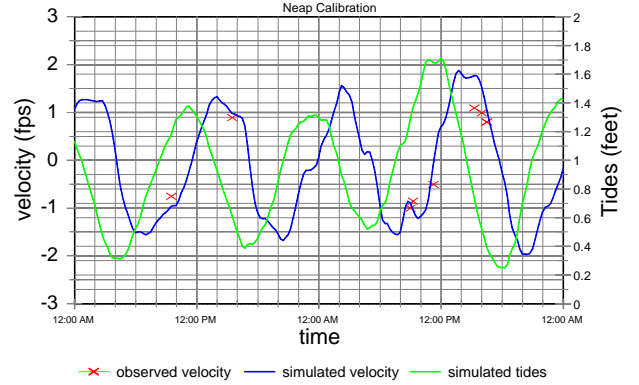
### 13 Corey Causeway B



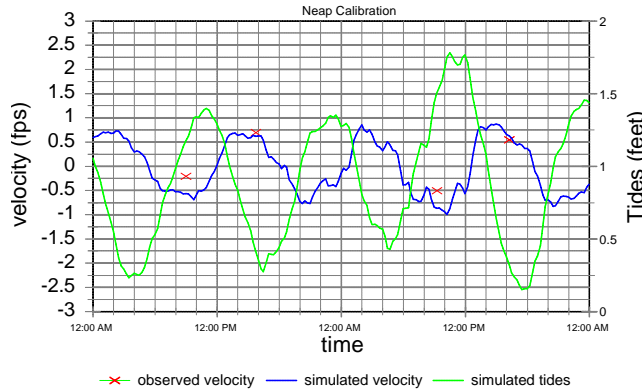
### 14 Corey Causeway C



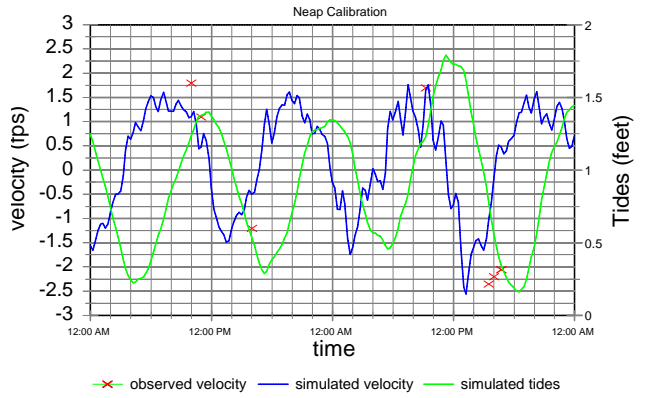
### 15 Vina del Mar E.



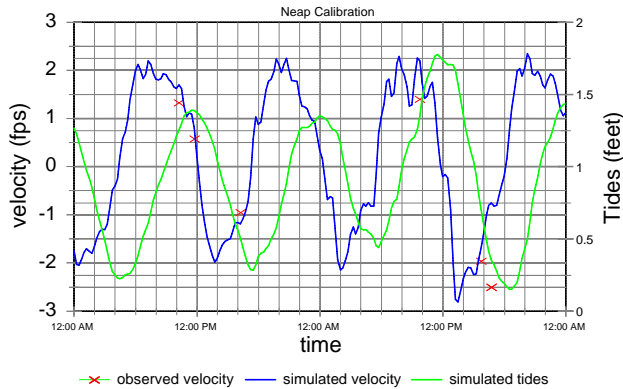
### 16 Vina del Mar W.



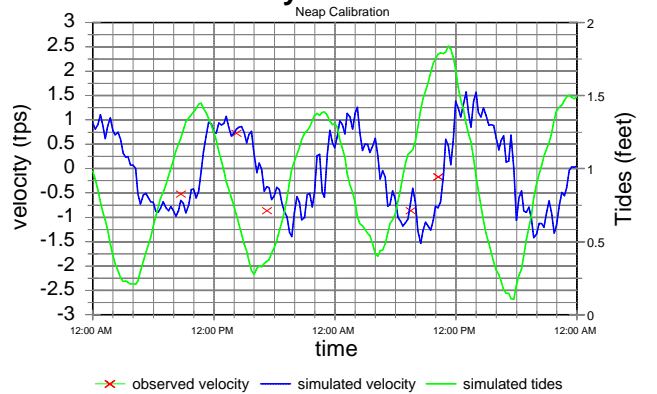
### 17 Isla del Sol



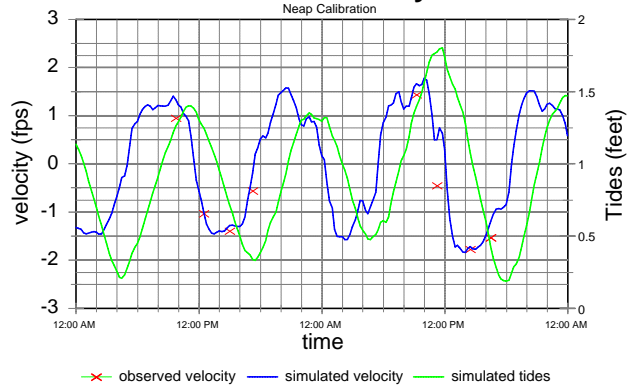
### 18 Cat's Point



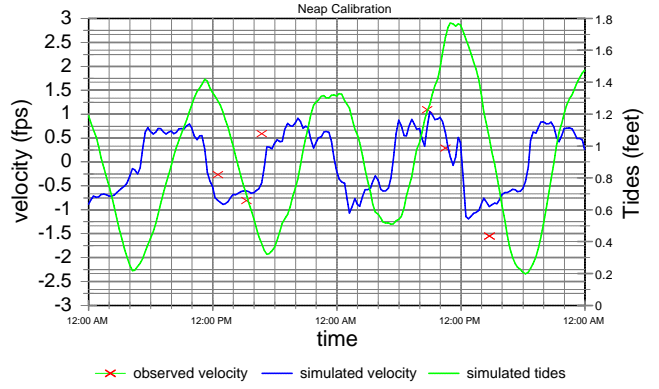
### 3C Crystal Island C



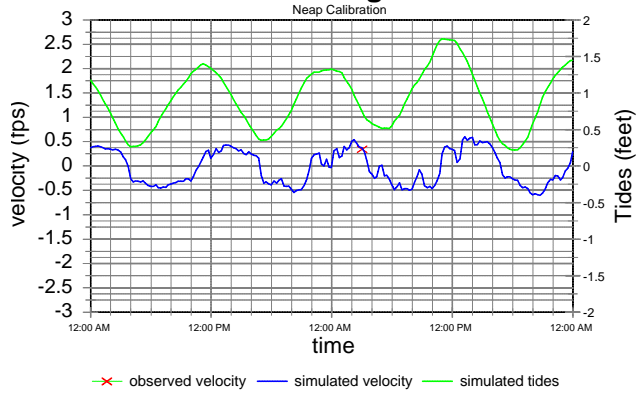
### 10A South Causeway Isl. S.



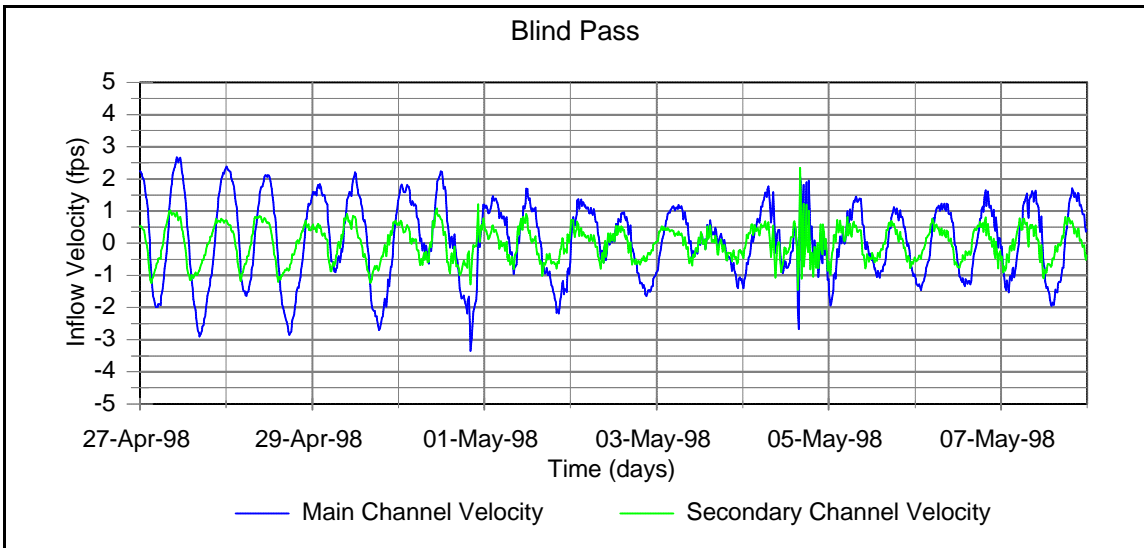
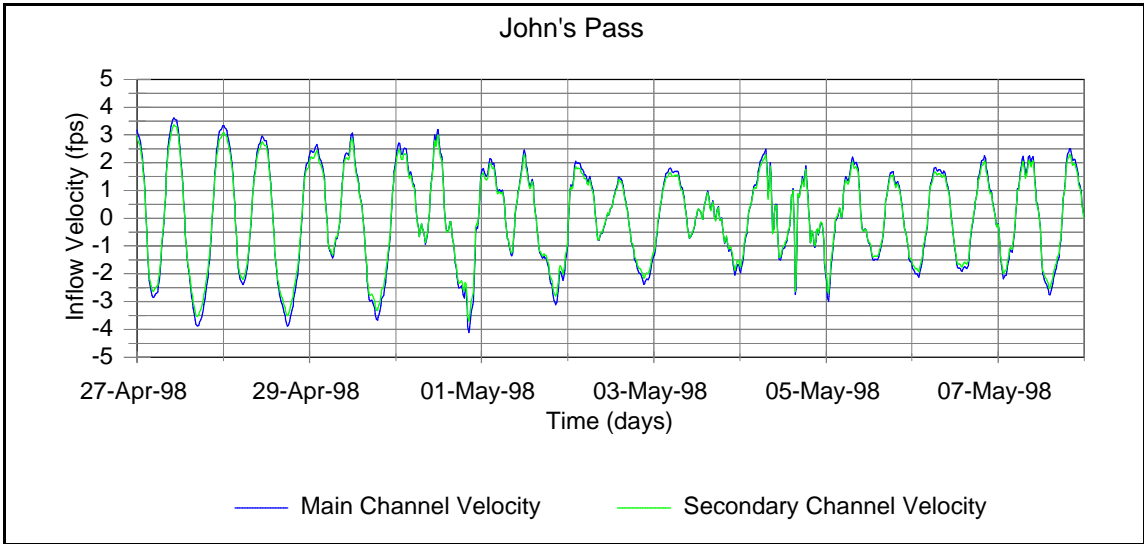
### 14A Pasadena Island



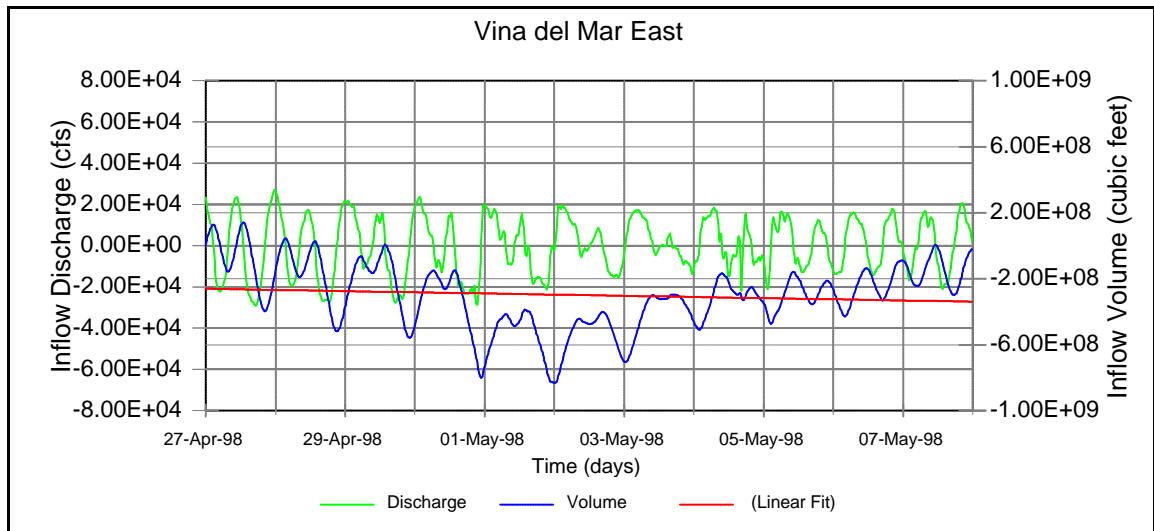
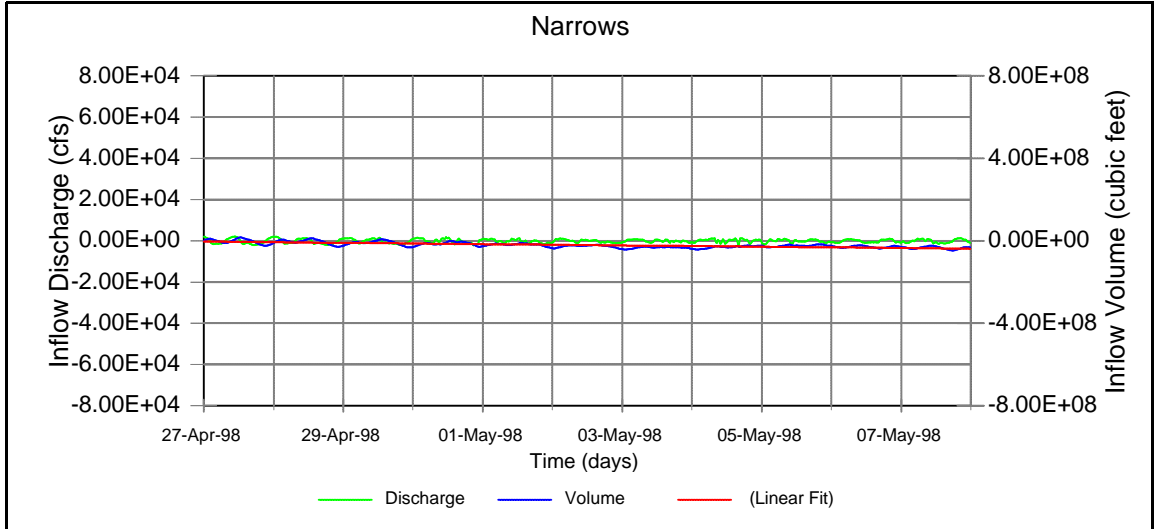
### 15A Boca Ciega Island



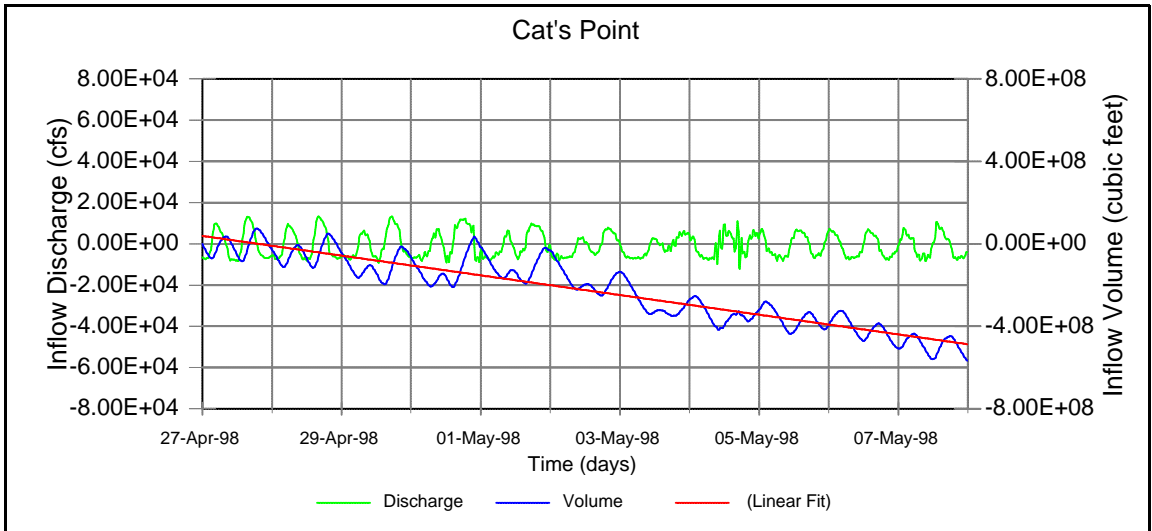
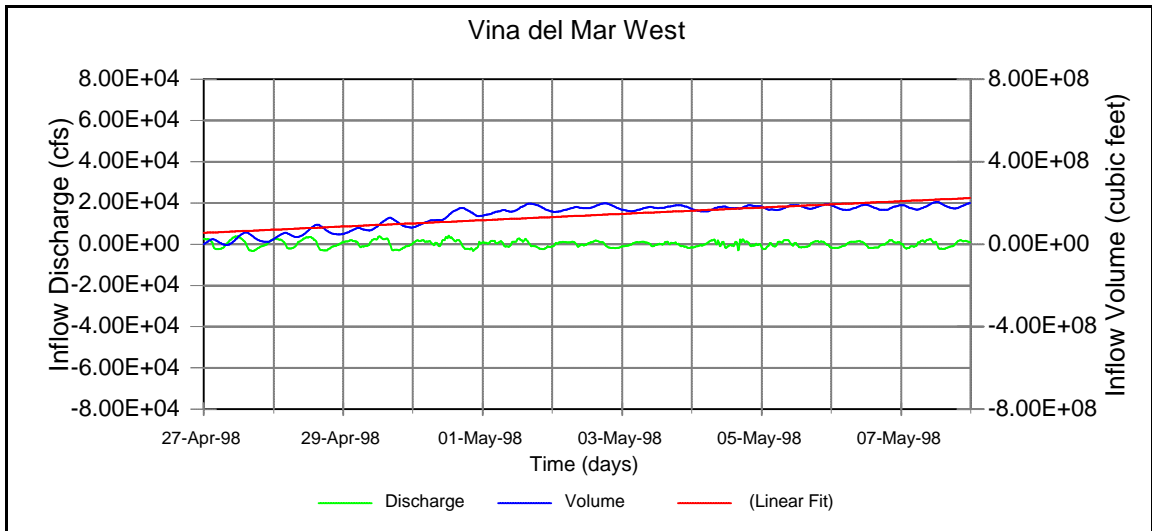
Appendix D. Channel Velocities at John's Pass and Blind Pass



Appendix E. Discharge, Volume, and Net Flow at Boundary Channels



Appendix E. (Continued).



Appendix E. (Continued)

